J. Fluid Mech. (1991), *vol.* 227, *pp.* 641–666
Printed in Great Britain

On strongly nonlinear vortex/wave interactions in boundary-layer transition

By P. HALL[1]† AND F. T. SMITH[2]

[1] Mathematics Department, The University, Exeter EX4 4QE, UK

[2] Mathematics Department, University College, Gower Street, London WC1E 6BT, UK

(Received 6 February 1990 and in revised form 5 December 1990)

The interactions between longitudinal vortices and accompanying waves considered here are strongly nonlinear, in the sense that the mean-flow profile throughout the boundary layer is completely altered from its original undisturbed state. Nonlinear interactions between vortex flow and Tollmien–Schlichting waves are addressed first, and some analytical and computational properties are described. These include the possibility in the spatial-development case of a finite-distance break-up, inducing a singularity in the displacement thickness. Second, vortex/Rayleigh-wave nonlinear interactions are considered for the compressible boundary layer, along with certain special cases of interest and some possible solution properties. Both types, vortex/Tollmien–Schlichting and vortex/Rayleigh, are short-scale/long-scale interactions and they have potential applications to many flows at high Reynolds numbers. Their strongly nonlinear nature is believed to make them very relevant to fully fledged transition to turbulence.

1. Introduction

The majority of any transition process from laminar to turbulent flow poses a considerable theoretical challenge since fully fledged transition is a strongly nonlinear process, i.e. it completely alters the mean-flow profile from its original laminar state. Much interest has therefore arisen recently in nonlinear three-dimensional interactions between longitudinal vortices and accompanying nonlinear waves, because of the strongly nonlinear nature of vortex/wave interactions and hence their likelihood of increased relevance to fully fledged transition, e.g. as observed experimentally by Klebanoff, Tidstrom & Sargent (1962), Hama & Nutant (1963), Nishioka, Asai & Iida (1981), Nishioka & Asai (1984, 1985), Kachanov & Levchenko (1984), Williams, Fasel & Hama (1984), Williams (1987), Thomas (1987) and simulated computationally by Wray & Hussaini (1984), Kleiser & Schumann (1984), Gilbert & Kleiser (1986, 1988), Zang & Hussaini (1986, 1987), Fasel, Rist & Konzelmann (1987), Spalart & Yang (1987), Laurien & Kleiser (1989), Zang & Krist (1989). In this work vortex/wave interactions are considered theoretically in the context of boundary-layer transition.

In the case of flat-surface boundary layers, there appear to be three main theories developed so far, of a truly nonlinear as well as rational nature: first, for nonlinear Tollmien–Schlichting (TS) interactions via triple-deck-like theory (e.g. Smith 1979*a*, 1986, 1988, 1991; Hall & Smith 1984; Duck 1985; Hoyle, Smith & Walker 1991); second, for nonlinear Euler interactions (Smith & Burggraf 1985; Smith & Stewart

† Current address: Mathematics Department, The University, Manchester, M13 9PL, UK.

1987; Smith, Doorly & Rothmayer 1990); and, third, for nonlinear vortex/wave interactions (Hall & Smith 1988, 1989, 1990; Bennett, Hall & Smith 1991; Smith & Walton 1989; Bassom & Hall 1990). The third, which is our concern here, can be regarded as stemming from the first, as Smith & Walton (1989) show. Alternatively, in the presence of curvature, longitudinal vortices are able to exist without any forcing from a wave system (Hall 1982; Hall & Lakin 1988; Hall & Seddougui 1989). Here it is found that strongly nonlinear vortex flows completely restructure the boundary layer in a manner which renders it neutrally stable to streamwise vortices; the latter result is closely related to the ideas of Malkus (1956) who proposed a 'marginal theory of turbulence.' All the above theories, for high Reynolds numbers, are known to be interconnected in that triple-deck interactions can lead on to Euler-stage flow (see Smith & Burggraf) and to vortex/wave interactions (see Hall & Smith 1988; and Smith & Walton 1989), and further likely connections are found to arise in this study. All are particularly attractive because they can produce substantial alterations of the mean-flow profile or shear in the boundary layer, in contrast to linear instability theory and weakly nonlinear theory (e.g. Stuart 1960 – Watson 1960 -like, Benney & Lin 1960, resonant triads (Craik 1971; Smith & Stewart 1987), critical-layer analyses, and associated near-linear-neutral analyses) where some interesting low-amplitude phenomena can be predicted but nevertheless the mean-flow quantities are little changed. Again, the truly nonlinear interactions above are based on rational arguments as distinct from the interesting but *ad hoc* approaches of certain other theories, while the largeness of the Reynolds number taken throughout seems not unlikely to be appropriate to the experimental range of greatest concern. The question of which strongly nonlinear interaction applies in any particular experimental configuration depends on the amplitudes and spectra of the input, at an initial time and/or position. In particular, the present vortex/wave interactions apply for waves of small amplitude which nevertheless are able to alter the mean-flow quantities because of the relatively short wavelength, compared with the relatively large development length of the mean flow, thus inducing full nonlinearity.

The aim in this work is to describe distinct cases of vortex/wave interaction in boundary-layer flows, as well as some interesting and useful sub-cases, of which there are many. We summarize the derivations from underlying flow structures and the governing equations, for a number of vortex/wave interactions, to focus attention on the wide range of possibilities and applications, and some solution properties are also given in the form of linear, secondary instability, weakly nonlinear, fully nonlinear similarity-type, and nonlinear breakdown phenomena, along with computational studies, as a start. A main task here however is felt to be to put the typical controlling equations of strongly nonlinear vortex/wave interaction on record, as they are believed to be of much significance and of broad application (see below).

The scales and amplitudes of the vortex flows tend to be relatively simple on the whole and can be inferred from the early Taylor-vortex calculations by Davey (1962), say, whereas the waves' scales and amplitudes are usually more involved. The origins of these scales and of the corresponding flow structures are to be found in the flow properties described by Hall & Smith (1984, 1988, 1989, 1990), Bennett *et al.* (1991), Smith & Walton (1989), for lower-amplitude interactions, and there is possible overlap with the work done independently by Benney & Chow (1989 and see references therein), granted certain questions on rationality. The two major kinds of nonlinear vortex/wave interaction that emerge, and are addressed below, concern what are effectively TS waves and Rayleigh waves.

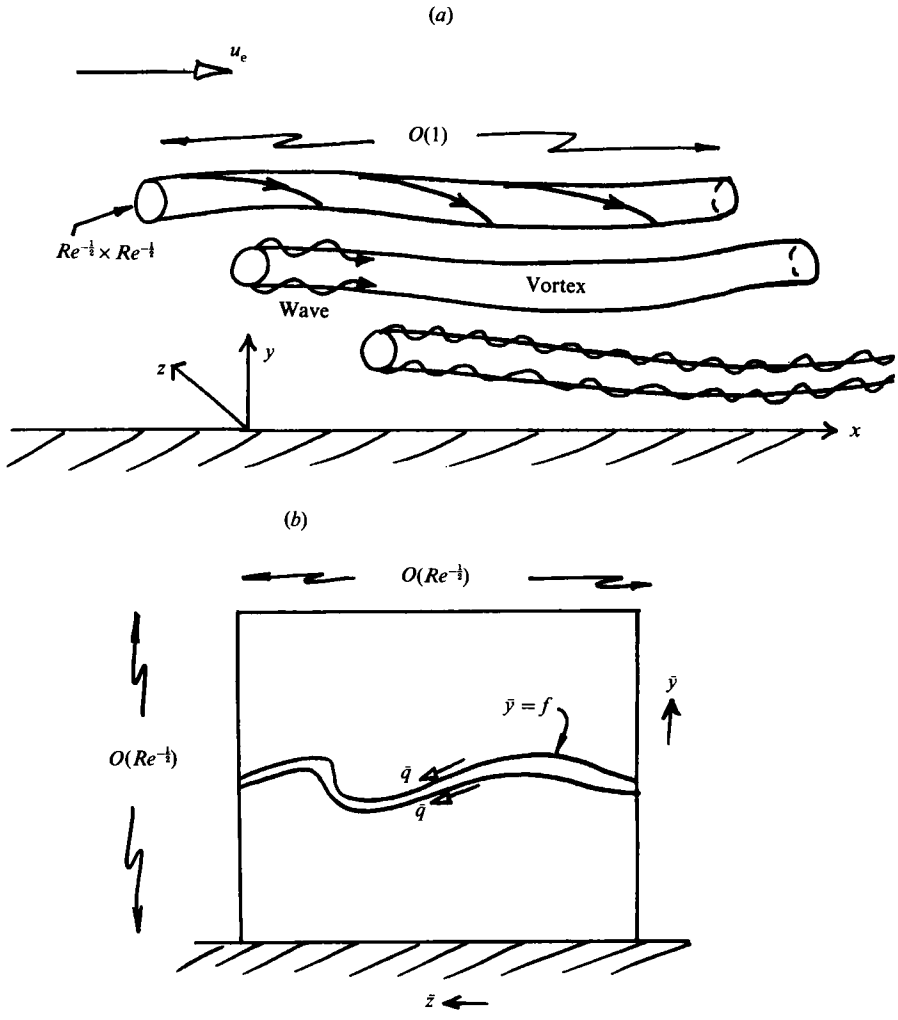

FIGURE 1. (*a*) Typical strongly nonlinear vortex/wave interactions in a boundary layer. The scales of the slowly varying vortices are shown for square vortices as in (2.6), (2.9), (4.1); the travelling waves present are either TS waves (§§2, 3) or Rayleigh waves (§§ 4, 5). Other scales possible are described in §2, specifically those of 'wide' and 'small' vortices in (2.1) and (2.12) respectively. (*b*) Cross-section $O(Re^{-\frac{1}{8}} \times Re^{-\frac{1}{4}})$ in the vortex/Rayleigh-wave case of §§4, 5, including the critical-layer ($O(Re^{-\frac{1}{8}})$ thick) effect at $\bar{y} = f$.

Vortex/TS-wave interactions are discussed in §2 (see also figure 1), where the scales, flow structure and controlling equations are presented, and in §3 where certain solution properties are considered. This is mainly for the incompressible boundary layer although the corresponding compressible version follows the same pattern, cf. Smith (1989), Blackaby (1991), Smith & Walton (1989). Vortex/Rayleigh-wave interactions (again see figure 1) are then described in §§4 and 5 for compressible boundary layers, given the earlier groundwork, and given the susceptibility of such boundary layers to Rayleigh waves, with the incompressible and other limiting regimes then being obtainable as special cases (see §5 and Appendix C). A number of interesting nonlinear flow properties seem to be suggested. These include the possibilities that the vortex/TS interaction can provide a lead into vortex/Rayleigh interaction, even in the incompressible regime, that either interaction can produce

eventually an Euler-stage flow, within a finite distance in the spatial problem or within a finite time for the temporal case (these distances and times being measured in the relatively slower-scale variables), that many waves can be activated together, and that successive shorter-scale vortex/wave interactions can be provoked, producing a cascade of scales. In addition, as the whole boundary layer is changed substantially in any of these nonlinear interactions, there is potential relevance to by-pass transition throughout as well as to more gradual transitions triggered initially by linear disturbances. Further comments are presented in §6.

The nonlinear vortex/wave interactions studied here also hold for many other flows in principle and have numerous applications. Examples are channel flows (see also Bassom & Hall 1990; Bennett *et al.* 1991), pipe flows (see also Walton 1991), wakes, plane Couette flow, water motions, e.g. Langmuir circulations, free shear layers, separations, flow over surface roughnesses, vortex breakdown, and possibly other rotating fluid flows. The vortex-wave interaction seems to apply in fact to any flow that admits relatively short-scale waves. Among the interactions, those of §4 for nonlinear Rayleigh-like waves would appear to have the broadest application.

In the following, the large Reynolds number Re is the global one, based on the airfoil chord and free-stream speed in the aerodynamic context, as are the corresponding non-dimensional coordinates x, y, z and velocities u, v, w, streamwise, normal and spanwise respectively for flat-surface flow, and the time t. Similarly, the non-dimensional density, viscosity, temperature and pressure are ρ, μ, T, p (with free-stream value p_∞), while M_∞, σ, C denote in turn the free-stream Mach number, the Prandtl number, and the constant in the Chapman viscosity law which is assumed for definiteness. The characteristic boundary-layer thickness is then $O(Re^{-\frac{1}{2}})$ in terms of $y(= Re^{-\frac{1}{2}}\bar{y})$, and the standard TS scalings (Smith 1979*a* and subsequent references as above), i.e. three-dimensional triple-deck with y for instance scaled as $\frac{3}{8}, \frac{1}{2}, \frac{5}{8}$ powers of Re^{-1} and x, z as $\frac{3}{8}$ powers, apply in the setting of §2, whereas standard Rayleigh scales of $\frac{1}{2}$ powers in x, y, z apply for §4. Throughout, the motions being considered are three-dimensional and unsteady.

2. Nonlinear vortex/Tollmien–Schlichting interactions

The vortex/TS nonlinear interactions that we address first here are larger-scale ones, in which the mean-flow profile of the entire $O(Re^{-\frac{1}{2}})$ boundary layer is altered from its original laminar form. We start with the *wide vortex*. The scales involved may be derived from an order-of-magnitude reasoning as follows. The small TS waves of typical pressure amplitude $\bar{\Pi}$ say, to be determined, have the triple-deck structure, so that their streamwise and spanwise velocity perturbations are of order $Re^{-\frac{1}{8}}h$ within the lower deck near the surface, where $\bar{\Pi} = Re^{-\frac{1}{4}}h$ and h is assumed to be small. The powers of the Reynolds number present here are those characteristic of the triple-deck, and hence of two- and three-dimensional TS waves, as set out in numerous previous works on TS waves alone: see references in the second paragraph of §1 and Appendix A. In particular the z-scale is comparable with $Re^{-\frac{3}{8}}$. Forcing of the near-surface vortex flow then occurs at the amplitude-squared level, including a vortex spanwise velocity of order $Re^{-\frac{1}{8}}h^2$, due to an expansion proceeding in powers of h. This velocity grows logarithmically at the edge of the lower-deck sublayer, as described by Hall & Smith (1989), and so it is little different in the main part of the boundary layer, the main deck. There the typical vortex dynamics is controlled by the convective–viscous balance acting on the $O(1)$ scale in x and hence, by continuity, since the z-scale is of order $Re^{-\frac{3}{8}}$, the representative w in the vortex has size $O(Re^{-\frac{3}{8}})$,

given that the streamwise velocity is of order unity. So nonlinear interaction arises when this size of spanwise velocity is comparable with that forced by the presence of the TS waves, i.e. with the order $Re^{-\frac{1}{8}}h^2$ (times $\frac{1}{8}\ln Re$ in view of the $\frac{1}{8}$-power difference between the lower- and main-deck scalings), from above. The critical size is therefore $h \sim Re^{-\frac{1}{8}}$ (times $\hat{\mathscr{L}} \equiv (\frac{1}{8}\ln Re)^{-\frac{1}{2}}$), corresponding to the pressure amplitude $\bar{\Pi} = Re^{-\frac{3}{8}}$ [times $\hat{\mathscr{L}}$] and confirming the relative smallness of the TS waves, which contrasts with their substantial impact on the main boundary-layer motion. The same estimate of size results from direct extensions of our previous work on related vortex/wave interactions (see references). The back effect of the induced longitudinal vortex motion on the waves themselves is felt through the streamwise skin friction which helps to control the waves' response within the sublayer.

The expansions of the flow solutions in the lower, main, and upper decks may then be set down, accounting for the extra logarithmic terms necessary in view of the logarithmic sublayer behaviour of the vortex spanwise velocity mentioned above. The unknown vortex or mean-flow velocity has the form

$$[u, v, w] = [\bar{u}, Re^{-\frac{1}{2}}\bar{v}, Re^{-\frac{3}{8}}\bar{w}] + \ldots \tag{2.1a}$$

across the majority of the boundary layer, while the wave velocity and pressure are

$$[u,v,w] = \begin{cases} O[Re^{-\frac{3}{8}}\hat{\mathscr{L}}], & \hat{\mathscr{L}} = (\frac{1}{8}\ln Re)^{-\frac{1}{2}}, \\ O[Re^{-\frac{1}{4}}, \quad Re^{-\frac{3}{8}}, \quad Re^{-\frac{3}{8}}]\hat{\mathscr{L}}, \\ O[Re^{-\frac{1}{4}}, \quad Re^{-\frac{1}{2}}, \quad Re^{-\frac{1}{4}}]\hat{\mathscr{L}}, \end{cases} \qquad p = \begin{cases} Re^{-\frac{3}{8}}\hat{\mathscr{L}}\tilde{p}_1, & (2.1b) \\ Re^{-\frac{3}{8}}\hat{\mathscr{L}}P_1, & (2.1c) \\ Re^{-\frac{3}{8}}\hat{\mathscr{L}}P_1, & (2.1d) \end{cases}$$

in the upper, main, and lower decks respectively. Here the variables in (2.1*a*) are independent of the fast scales X, $\tilde{t}$, whereas those in (2.1*b–d*) depend on X, $\tilde{t}$, where $x = Re^{-\frac{3}{8}}X, t = Re^{-\frac{1}{4}}\tilde{t}$ and the multiple scaling

$$\partial_x \to Re^{\frac{3}{8}}\partial_X + \partial_x, \quad \partial_t \to Re^{\frac{1}{4}}\partial_{\tilde{t}} + \partial_t$$

operates. Also, the wave pressure P_1 is independent of $\bar{y}$, and the main timescale of the wave is $O(Re^{-\frac{1}{4}})$, corresponding to a non-dimensional frequency of $O(Re^{\frac{1}{4}})$. See figure 1. More details on the nature of the expansions are in Appendix A. The resulting governing equations for the vortex/wave interaction in this context are therefore:

vortex

$$\bar{u}_x + \bar{v}_{\bar{y}} + \bar{w}_Z = 0, \tag{2.2a}$$

$$\bar{u}_t + \bar{u}\,\bar{u}_x + \bar{v}\,\bar{u}_{\bar{y}} + \bar{w}\,\bar{u}_Z = -\bar{p}'(x) + \bar{u}_{\bar{y}\bar{y}} \tag{2.2b}$$

$$\bar{w}_t + \bar{u}\,\bar{w}_x + \bar{v}\,\bar{w}_{\bar{y}} + \bar{w}\,\bar{w}_Z = 0 + \bar{w}_{\bar{y}\bar{y}}, \tag{2.2c}$$

subject to

$$\bar{u} = \bar{v} = 0, \quad \bar{w} = -\bar{\lambda}^{-2}\partial_Z(|P|^2 + \alpha^{-2}|P_Z|^2) \quad \text{at} \quad \bar{y} = 0, \tag{2.2d}$$

$$\bar{u} \to u_e(x), \quad \bar{w} \to 0 \quad \text{as} \quad \bar{y} \to \infty; \tag{2.2e}$$

wave

$$P_{ZZ} - \mathscr{F}(\bar{\lambda}_Z/\bar{\lambda})P_Z - \alpha^2 P = \mathscr{G}A, \tag{2.3a}$$

with

$$\bar{\lambda} = \bar{u}_{\bar{y}} \quad \text{at} \quad \bar{y} = 0. \tag{2.3b}$$

Here the scaled vortex velocity $(\bar{u}, \bar{v}, \bar{w})$ and skin friction $\bar{\lambda}$, and the wave pressure P and displacement $-A$, are all unknown, as is the (real) wavenumber $\alpha(x)$ if the spatial development is under consideration, and $P_1 = PE + \text{c.c.}$ with $E \equiv \exp(\mathrm{i}\alpha X - \mathrm{i}\Omega\tilde{t})$ (see next paragraph). Also, $\bar{p}'(x) = -u_e u_e'(x)$ is the prescribed external

pressure gradient, if any, and the spanwise scale has $z = Re^{-\frac{3}{8}}Z$. The wave pressure-displacement (P–A) law required to complete the system is given by solving

$$(\partial_{\tilde{y}}^2 + \partial_Z^2 - \alpha^2)\,\tilde{p} = 0, \tag{2.4a}$$

with

$$\tilde{p} \to 0 \quad \text{in the far field,} \tag{2.4b}$$

$$\tilde{p} \to P, \quad \tilde{p}_{\tilde{y}} \to -\alpha^2 u_e^2 A \quad \text{as} \quad \tilde{y} \to 0+, \tag{2.4c}$$

for the upper-deck response in the potential flow just outside the boundary layer, in the present incompressible regime. The coefficients appearing in (2.3a) are defined by

$$\mathscr{F} = \frac{3}{2} + \frac{\xi_0 \operatorname{Ai}'(\xi_0)}{2\operatorname{Ai}(\xi_0)}\left(1 + \frac{\kappa\xi_0}{\operatorname{Ai}'(\xi_0)}\right), \quad \mathscr{G} = (\mathrm{i}\alpha\bar{\lambda})^{\frac{5}{3}} \operatorname{Ai}'(\xi_0)/\kappa, \tag{2.5a, b}$$

$$\xi_0 = -\frac{\mathrm{i}^{\frac{1}{3}}\Omega}{(\alpha\bar{\lambda})^{\frac{2}{3}}}, \quad \kappa = \int_{\xi_0}^{\infty} \operatorname{Ai}(q)\,\mathrm{d}q, \tag{2.5c–d}$$

where Ai is the Airy function and, for the spatial case again, Ω (real) is the constant, imposed, scaled frequency. We should emphasize that both the wavenumber α and the frequency Ω are to remain real throughout, i.e. the mean flow has to adjust to keep the wave part in neutral. Growing modes, in contrast, would tend to lead into a pure TS nonlinear stage as referred to in §1 (yielding in particular the nonlinear break-up of Smith (1988), as in Hoyle, Smith & Walker (1991), Peridier, Smith & Walker (1991), and see later); while, again, our earlier work (e.g. Hall & Smith 1988) on vortex/wave interactions indicates examples where such mode growth is suppressed nonlinearly in favour of vortex/wave interaction of the present kind. In the work of Benney & Chow it is not clear that the wave system driving the mean flow can ever be neutral.

The wave-forcing of the vortex motion appears in the effective spanwise surface velocity in (2.2d), an amplitude-squared effect anticipated in the first paragraph of this section. The vortex forcing of the wave, on the other hand, is through the skin-friction factor $\bar{\lambda}$ in the TS pressure equation (2.3a). In the pure spatial-development problem the terms $\bar{u}_t$, $\bar{w}_t$ in (2.2b, c) are to be omitted, and, in the background, the short-scale wave is dependent on X through the form $P(x, Z)E + \text{c.c.}$ in effect while the long-scale vortex flow is independent of X (more formally, $\mathrm{i}\alpha X$ should be replaced by $\mathrm{i}\int \alpha\,\mathrm{d}x Re^{\frac{3}{8}}$). The main alternative of pure temporal development has ∂_x identically zero instead in (2.2a–c), along with the multi-scaling above where the fast-scale wave varies with $\tilde{t}$ as above, i.e. we have $P(t, Z)E + \text{c.c.}$ in effect, but the slow-scale vortex evolution is independent of $\tilde{t}$, and α is then constant with $\Omega(t)$ to be determined.

The wide-vortex/TS interaction, then, is governed by (2.2)–(2.4).

The next two types of vortex/wave nonlinear interaction addressed are for the *square vortex*, for which the y- and z-scales of the vortex are comparable, of order $Re^{-\frac{1}{2}}$. These types have scales implied to some extent by Bennett & Hall (1987) and by an examination of the wide-vortex case above for condensed $|z|$ scales. First, the slowly varying square vortex has the form

$$[u, v, w] = [\bar{u}, Re^{-\frac{1}{2}}\bar{v}, Re^{-\frac{1}{2}}\bar{w}], \quad p = \bar{p}(x) + Re^{-1}\bar{p}_2 + \ldots \tag{2.6a}$$

with $z = Re^{-\frac{1}{2}}\bar{z}$ and $\bar{z}$ of $O(1)$, and the fast-varying wave disturbance is now condensed inside the boundary layer, such that its velocity and pressure fields have

$$[u, v, w, p] = \begin{cases} O[Re^{-\frac{1}{2}}]\,\mathscr{L}_1, \quad \mathscr{L}_1 = (\frac{1}{6}\ln Re)^{-\frac{1}{2}}, & (2.6b) \\ O[Re^{-\frac{1}{3}},\ Re^{-\frac{1}{2}},\ Re^{-\frac{1}{3}},\ Re^{-\frac{1}{2}}]\,\mathscr{L}_1 & (2.6c) \end{cases}$$

in the midst of the boundary layer and in the $O(Re^{-\frac{2}{3}})$ sublayer, in turn. Also, $\partial_x \to Re^{\frac{1}{2}}\partial_X + \partial_x$. So here the vortex equations are

$$\bar{u}_x + \bar{v}_{\bar{y}} + \bar{w}_{\bar{z}} = 0, \tag{2.7a}$$

$$\bar{u}_t + \bar{u}\,\bar{u}_x + \bar{v}\,\bar{u}_{\bar{y}} + \bar{w}\,\bar{u}_{\bar{z}} = -\bar{p}'(x) + \bar{u}_{\bar{y}\bar{y}} + \bar{u}_{\bar{z}\bar{z}}, \tag{2.7b}$$

$$\bar{v}_t + \bar{u}\,\bar{v}_x + \bar{v}\,\bar{v}_{\bar{y}} + \bar{w}\,\bar{v}_{\bar{z}} = -p_{2\bar{y}} + \bar{v}_{\bar{y}\bar{y}} + \bar{v}_{\bar{z}\bar{z}}, \tag{2.7c}$$

$$\bar{w}_t + \bar{u}\,\bar{w}_x + \bar{v}\,\bar{w}_{\bar{y}} + \bar{w}\,\bar{w}_{\bar{z}} = -p_{2\bar{z}} + \bar{w}_{\bar{y}\bar{y}} + \bar{w}_{\bar{z}\bar{z}}. \tag{2.7d}$$

These are the nonlinear Görtler-vortex equations in a boundary layer at zero Görtler number (Hall 1988); in the presence of curvature a term proportional to $\bar{u}^2$ must be inserted in (2.7*c*). The boundary conditions appropriate to (2.7*a–d*) are

$$\bar{u} = \bar{v} = 0, \quad \bar{w} = -\bar{\lambda}^{-2}\partial_{\bar{z}}[|P|^2 + \alpha^{-2}|P_{\bar{z}}^2|] \quad \text{at} \quad \bar{y} = 0, \tag{2.7e}$$

$$\bar{u} \to u_e(x) \quad \text{as} \quad \bar{y} \to \infty, \tag{2.7f}$$

while the coupled wave-pressure equation is

$$P_{\bar{z}\bar{z}} - \mathscr{F}(\bar{\lambda}_{\bar{z}}/\bar{\lambda})\,P_{\bar{z}} - \alpha^2 P = 0. \tag{2.8}$$

Here $\bar{\lambda}$ is the unknown skin friction as defined in (2.3*b*) and $\mathscr{F}$ is as in (2.5*a*), but now the interaction relation of (2.4) is replaced by $A \to 0$ effectively. This new feature is due to the shortened streamwise and spanwise lengthscales associated with the wave, both of which are now $O(Re^{-\frac{1}{3}})$, thus suppressing the inviscid pressure feedback from outside the boundary layer. The timescale of the wave is now $O(Re^{-\frac{1}{3}})$, i.e. the frequency is $O(Re^{\frac{1}{3}})$, larger than before. The other new features of the present two-tier structure, for the square-vortex case, are the balance of normal and spanwise diffusion, in (2.7*b–d*), and the interpretation of (2.7*c*, *d*) as a streamwise vorticity equation (on elimination of p_2 by cross-differentiation). It should be noted however that (2.8) has no solutions with α real if $\bar{\lambda}_{\bar{z}} = 0$, and even with $\bar{\lambda}_{\bar{z}} \neq 0$ the possibility exists that there are no solutions of the full interactive equations in this case.

The other type of nonlinear interaction involving a square vortex has some analogies with that of Bennett *et al.* (1991) for channel flow. Here the vortex exhibits scales as in (2.6*a*) again, but the wave form is distinct from (2.6*b*, *c*) in that the triple-deck structure is reinstated, such that

$$[u, v, w, p] = O(Re^{-\frac{3}{8}})\,\hat{\mathscr{L}} + O(Re^{-\frac{5}{8}})\,\hat{\mathscr{L}} \tag{2.9a}$$

in the upper deck, and so on: in particular

$$p = (Re^{-\frac{3}{8}}P_0 + \ldots + Re^{-\frac{5}{8}}P_1)\,\hat{\mathscr{L}} + \ldots \tag{2.9b}$$

in the main and lower decks, and similarly in the upper deck, with $P_0(x)$ uniform in $\bar{z}$ but P_1 depends on $x, \bar{z}$. The relative contributions of order $Re^{-\frac{1}{4}}$ in the wave form affect both the vortex and the TS response throughout. Thus the vortex equations are again (2.7*a–f*) except that the spanwise slip condition in (2.7*e*) is replaced by

$$\bar{w} = -\bar{\lambda}^{-2}\partial_{\bar{z}}[P_0 P_1^* + P_0^* P_1 + \alpha^{-2}|P_{1\bar{z}}|^2] \quad \text{at} \quad \bar{y} = 0, \tag{2.10}$$

and the wave-pressure equation becomes now

$$P_{1\bar{z}\bar{z}} - \mathscr{F}(\bar{\lambda}_{\bar{z}}/\bar{\lambda})\,P_{1\bar{z}} - \alpha^2 P_0 = \mathscr{G}A_0, \tag{2.11}$$

where $A_0 = \alpha^{-1}P_0$. Here again the y- and z-diffusion effects in the vortex motion are comparable, but the increase in the skin-friction variation across the span, relative to the wide-vortex case, causes the splitting of the TS wave response as in (2.9*b*). The solution of (2.11) for P_1 can be written in integral form as in Bennett *et al.* and

substituted into the slip condition (2.10) in principle. Other scales and forms of splitting are also possible for this square-vortex type.

We move on now to the fourth type of nonlinear interaction to be considered, that for a *small vortex*. This arises as an interesting sub-case of the interaction (2.2)–(2.4), with the characteristic $\bar{y}$-scale reduced to $O(\Delta)$ say, near the surface, where the new parameter $\Delta \ll 1$. So we might expect that $\bar{u} \sim \Delta$, in an $O(\Delta)$ sublayer, with the x-scale reduced to the order Δ^3 to preserve the convective–viscous balance in (2.2). Hence by continuity $\bar{v}$ is large, $O(\Delta^{-1})$, and $\bar{w}$ is still larger, $O(\Delta^{-2})$, provided the Z-scale remains intact. The nonlinear interplay between the vortex and the wave also stays intact if the scaled wave pressure P is increased by an amount Δ^{-1}, from (2.3), with α remaining $O(1)$. So here the vortex quantities are

$$[u, v, w] = O[\Delta, Re^{-\frac{1}{2}}\Delta^{-1}, Re^{-\frac{3}{8}}\Delta^{-2}] \quad \text{with} \quad \bar{y} \sim \Delta, x \sim \Delta^3, \tag{2.12a}$$

and the TS wave pressure is increased to

$$p = O(Re^{-\frac{3}{8}}\Delta^{-1}), \tag{2.12b}$$

to within a logarithmic factor. The governing equations for this case, in scaled form, are (2.2) with $\bar{p}'(x)$ absent and with (2.2e) replaced by

$$\bar{u}_{\bar{y}} \to \lambda_1 \quad \text{as} \quad \bar{y} \to \infty, \tag{2.13}$$

in effect, coupled with (2.3), (2.4) again. Here the constant λ_1 is the skin-friction factor for the undisturbed incident boundary layer. As Δ tends back towards $O(1)$ the wide-vortex case of (2.2)–(2.4) is approached, whereas for Δ reduced towards $O(Re^{-\frac{1}{8}})$ the small-scale interaction of Smith & Walton (1989) is recovered. A number of other small-vortex/wave nonlinear interactions can be derived in similar vein from the previous ones.

All the vortex/wave interactions described above are fully nonlinear in the sense defined in §1. In general each one needs a computational treatment, marching forward in x from given starting conditions at $x = 0$, say, in the spatial-development setting, or forward in t from initial conditions at $t = 0$ for the temporal setting. Note however that for either the temporal or spatial problem we cannot arbitrarily choose the input vortex velocity field since the associated Tollmien–Schlichting wave must satisfy an eigenrelation dependent on the initial shear stress. Some solution properties are presented below.

3. Nonlinear interaction properties

Most of our interest here is in the spatial development for the wide vortex of (2.2)–(2.4) and for its small-vortex form (2.13). The nonlinear flow properties of the vortex/wave interactions seem to depend to a large extent on the amplitude and spectra of the input disturbance upstream.

Certain special cases may be addressed first, as guidelines. Thus if the input comprises two *oblique* waves of relatively low amplitude and spanwise wavenumbers $\pm\beta$ say, then an analysis for (2.13) for instance can be conducted similarly to, although with some differences from, the analysis in Hall & Smith (1989), when the latter is corrected for a logarithmic effect, like that in (2.1b), as described by Blennerhassett & Smith (1991). Such analysis yields interaction equations between the near-neutral waves' amplitudes and the induced vortex motion. The solutions of these weakly nonlinear equations in the Hall & Smith (1989) case show that, depending on β, either a finite-distance singularity is encountered or a far-

downstream asymptote with exponential growth is attained. In the present context, the former would tend to reinstate the full vortex/wave system associated with (2.13), whereas the latter would lead on eventually to the longer-scale vortex/wave interaction of (2.2)–(2.4). Similarly, if the input wave is *near-planar* then analysis along the lines of Smith & Walton (1989) can be applied initially. For relatively small amplitudes, the solution properties found with weak nonlinearity present again tend to reactivate (2.2)–(2.4) or (2.13) in full. For non-small amplitudes, pronounced secondary instability to three-dimensional modes is found, among other things, with the near-planar input, the three-dimensional components growing initially in a form analogous to the exponential of an exponential of distance.

The above cases could be used to provide upstream starting conditions for the full vortex/wave-interaction systems (2.2)–(2.4), (2.13), e.g. at finite or large negative x respectively. The ultimate downstream behaviour on the other hand for the small-vortex case is considered in Smith & Walton (1989), where three main possibilities are raised. One is that the full interaction continues to downstream infinity and acquires a nonlinear similarity form (with the scaled $\bar{u}, P, \bar{y}, \bar{w}$ behaving as scaled $x^{\frac{1}{3}}$, $x^{-\frac{1}{3}}$, $x^{\frac{1}{3}}$, $x^{-\frac{2}{3}}$ in turn), properties of which are given in Smith & Walton (1989) and by Walton (1991). In that event, the small-vortex/wave interaction acts as a precursor to the wide-vortex form. The second possibility concerns a three-dimensional strong-attachment singularity occurring in the vortex and wave solutions at finite x downstream. This typically takes the form, with $n > \frac{1}{2}$,

$$\bar{y} \sim (x_A - x)^n \bar{\bar{y}}, \quad \bar{v} \sim (x_A - x)^{-n}, \quad \bar{w} \sim (x_A - x)^{-2n}, \tag{3.1a}$$

on approach to a surface attachment line $x = x_A(Z) -$, say. Here $\bar{u}$ is typically $O(1)$. Near a valley plane $Z = Z_1$ for instance, where $\bar{w} \sim (Z - Z_1)\,\hat{w}(\bar{\bar{y}})$ vanishes, the cross-stream balances

$$\bar{v}_{\bar{\bar{y}}} + \hat{w} = 0, \quad \bar{v}\hat{w}_{\bar{\bar{y}}} + \hat{w}^2 = \hat{w}_{\bar{\bar{y}}\bar{\bar{y}}}$$

dominate, yielding the solutions

$$\bar{v} = \bar{\gamma}[\exp(-\bar{\gamma}\bar{\bar{y}}) - 1], \quad \hat{w} = \bar{\gamma}^2 \exp(-\bar{\gamma}\bar{\bar{y}}), \tag{3.1b}$$

where $\bar{\gamma}$ is a positive constant. Hence the wave-pressure amplitude P is proportional to $(x_A - x)^{-n}$ and also becomes singular at $x = x_A$. The 'strong attachment' here is associated with the decreasing $\bar{y}$-scale in (3.1a). The third possibility in Smith & Walton is again a finite-distance singularity but of a three-dimensional separation kind, taking place in the vortex motion, probably at a peak plane $Z = Z_2$ say. (The 'separation' is due to the increasing $\bar{y}$-scale in (3.2a) below). There

$$\bar{y} \sim (x_B - x)^{-N} Y, \quad \bar{u} \sim (x_B - x)^q U, \tag{3.2a, b}$$

$$\bar{v} \sim (x_B - x)^{-\Gamma}, \quad \bar{w} \sim (x_B - x)^{q-1}(Z - Z_2), \tag{3.2c, d}$$

with $N = \Gamma + q - 1$ positive and $q > 1 - 2\Gamma$, so that the local response is predominantly inviscid in a region which thickens in singular fashion as $x \to x_B -$. The solution has the form

$$\mathrm{d}U/\mathrm{d}Y = A_1 U^{m_1} + A_2 U^{m_2}, \quad m_1 = 1 + N/q, \quad m_2 = m_1 - 1/q, \tag{3.2e}$$

where A_1, A_2 are constants. For example, if $\Gamma = \frac{1}{2}$, $q = 1$, then $N = \frac{1}{2}$ and U takes a $(\tan)^2$ form; indeed, further work by F. T. Smith and A. G. Walton (see also Walton 1991) points to this example as being the *general* case for the separation singularity. The description (3.2a–e) holds for a finite range of Y, with U becoming singular at $Y = Y_1$ say in such a way that a thinner region of extent $O(1)$, in terms of $y - (x_B - x)^{-N} Y_1$, is induced to smooth out the velocity profiles. In this $O(1)$ region,

the velocities $\bar{u}, \bar{w}$ are $O(1)$ and their profiles are arbitrary, i.e. dependent on the flow history, apart from the matching with (3.2*e*) at the lower extremes and (2.13) for example in the upper extremes. In particular the effective boundary-layer displacement

$$\delta^* \sim (x_B - x)^{-N} \tag{3.2f}$$

becomes large in this separation singularity, including the favoured case $N = \frac{1}{2}$. This increase in the normal scale is connected perhaps with the formation of a lambda (loop) or hairpin vortex in practice, as Smith & Walton indicate, a connection which is further supported by the nearly separated or reversed form of the velocity profiles involved: see the reference above.

The proposed attachment singularity (3.1) and separation one (3.2) apply equally well to the wide-vortex case in principle. The similarity form mentioned previously does not apply, however, and appears at first sight to be replaced by the far-downstream behaviour

$$P \sim P_0 x^{-\frac{3}{4}} + P_1 x^{-\frac{5}{4}} + \ldots, \quad \alpha \sim \alpha_0 x^{-\frac{1}{4}}, \tag{3.3a, b}$$

$$\bar{u} \sim 1, \quad \bar{v} \sim x^{-\frac{1}{2}}, \quad \bar{w} \sim x^{-1}, \quad \lambda \sim x^{-\frac{1}{2}}, \tag{3.3c–f}$$

suggested by (2.2)–(2.4), at least if the Z-scale stays fixed at $O(1)$, as might occur with Z-periodicity present. Here P_0 is independent of Z, and the splitting in (3.3*a*) and the rest of the solution structure bear some resemblance to the square-vortex form in (2.9)–(2.11), although now $|\xi_0|$ is large ($\sim x^{\frac{1}{2}}$), so that relatively high-frequency features apply. Conversely, a low-frequency input with $\Omega \ll 1$ would produce the form in (3.3), downstream, with x replaced by Ω^{-2} in effect. Further investigation however suggests that there are no high-frequency solutions with $|\xi_0|$ large, e.g. from analysis of (2.3*a*) with (2.5*a–d*). Instead, the flow solution seems more likely to terminate with a finite-distance singularity, as in (3.1), (3.2) or with the wave-pressure amplitude tending to zero in a square-root fashion, in view of (2.2*d*), similar to a special case given in Smith & Walton (1989). Other possibilities for the wide-vortex and small-vortex nonlinear interactions with TS waves may exist of course, and likewise for the square-vortex forms in §2.

Computational studies have been made of both the wide- and the small-vortex/wave interactions of (2.2)–(2.4) and (2.13) respectively. Spectral treatments for the Z-variation have been applied to each case, and a finite-difference Z-representation has also been applied to the small-vortex case. These studies are being continued. Here we report on some preliminary but significant results obtained in our numerical investigation of the wide-vortex/wave interaction problem. This was done using a mixed finite-difference/spectral approximation to the vortex/wave equations (2.2) – (2.4). Thus, for example, $\bar{u}$ is written as

$$\bar{u} = \bar{u}_0(x, \bar{y}) + \sum_1^\infty \bar{u}_n(x, \bar{y}) \cos n\beta Z, \tag{3.4}$$

and the $x, \bar{y}$-dependencies of $\bar{u}_n$ are then approximated using finite differences. All of our calculations were for the zero-pressure-gradient case, $\bar{p}' = 0$, but the scheme as described could be carried out for pressure-gradient-driven boundary layers.

Suppose then that $\bar{u}, \bar{v}$ and $\bar{w}$ together with P and A, and α, Ω, are known at $x = \bar{x}$; we now describe a scheme which can be used to advance the solution to $x = \bar{x} + \epsilon$ in such a way that the wave frequency Ω is held fixed. Thus we are assuming that as the wave evolves its frequency stays constant whilst its wavelength and amplitude vary.

In order to step the solution forward, we decouple the vortex and wave equations

by making w at $x = \bar{x}+\bar{\epsilon}$ satisfy the required boundary condition at $\bar{y} = 0$ evaluated in terms of P known at $x = \bar{x}$. The x- and z-momentum equations for the combined mean flow–vortex field can then be stepped forward using essentially the scheme used by Hall (1988) in an investigation of fully nonlinear Görtler vortices. The reader is referred to that paper for precise details of that scheme. It suffices here to say that $\bar{y}$-derivatives are approximated using central differences and the nonlinear terms involving any harmonic content of $\bar{u}, \bar{v}$ and $\bar{w}$ are iterated upon until a converged solution is found.

The above procedure is used to advance the vortex velocity field to $x = \bar{x}+\bar{\epsilon}$ and the corresponding shear stress at that point can then be found from $\bar{u}$. The eigenrelation specified by (2.3a) and (2.4a–c) will, for fixed frequency, determine a complex value for the streamwise wavenumber α. However, it is implicit in our analysis that the wavenumber α is real, so that the eigenrelation at $x = \bar{x}+\bar{\epsilon}$ in general does not have an acceptable solution. At this stage there are two simple procedures which can be used to remedy the situation. Firstly, the value of $\bar{w}(\bar{y} = 0)$ at $x = \bar{x}+\bar{\epsilon}$ can be iterated upon in order to make α calculated at $\bar{x}+\bar{\epsilon}$ purely real. In effect this is most easily done by iterating upon some measure of the Tollmien–Schlichting wave amplitude at $x = \bar{x}+\bar{\epsilon}$. Alternatively, we proceed by writing (2.3a) in the form

$$\left\{P_{zz}-\frac{1}{2}\frac{\mathscr{F}\bar{\lambda}_z}{\bar{\lambda}}P_z-\alpha^2 P-\frac{\mathscr{G}A}{2}\right\}^+ = \left\{\frac{1}{2}\frac{\mathscr{F}\bar{\lambda}_z}{\bar{\lambda}}P_z+\frac{\mathscr{G}A}{2}\right\}^- \tag{3.5}$$

where $-$ and $+$ denote quantities evaluated at $\bar{x}$ and $\bar{x}+\bar{\epsilon}$ respectively. The right-hand side of (3.5) is then known, so that after expanding P in a Fourier series (3.5) can be solved for P at $\bar{x}+\bar{\epsilon}$. We note that this can be done for any value of α but a constraint on the wavenumber can in effect be found by further consideration of (2.3). Since that equation is linear we can at each step multiply the solution by a factor $e^{i\chi(x)}$ with χ to be found at higher order. Thus (2.3) must be solved with some condition imposed on its phase at a given value of Z. Without loss of generality we can make P real at $Z = 0$. The value of α used to determine P above is then iterated upon in order to make (say) $(P)_i = 0$ at $Z = 0$. In this procedure the Tollmien–Schlichting frequency is of course fixed and a value for α at $\bar{x}+\bar{\epsilon}$ is obtained.

The calculations which we report on have been carried out using the second of the procedures described above in order to keep α real. The input used to begin our calculations was found in the following way. Firstly, we assume some form for $\bar{u}$ at an initial value $x = x^*$ and then solve the eigenvalue problem determined by (2.3a), (2.4a–c) for the appropriate real values of α and Ω. The values of α and Ω calculated in this way depend on $\bar{u}$ through the wall shear $\bar{\lambda}$, so that for example an almost two-dimensional input Tollmien–Schlichting wave can be constructed by choosing $\bar{u}_n$ in (3.4) for $n \geqslant 1$ to be small compared with $\bar{u}_0$. Having solved for the Tollmien–Schlichting eigenrelation at $x = x^*$ the boundary condition to be satisfied by $\bar{w}$ then can be determined in terms of P. The initial profile for $\bar{w}$ at $x = x^*$ is then chosen to be consistent with this condition. In the calculations reported here $\beta = 0.02$, $x^* = 55$, and eight Fourier modes were retained in the Fourier expansion of the vortex and Tollmien–Schlichting fields. Note here that the local wavenumber at a given x is proportional to $x^{\frac{1}{2}}$ so that the chosen value of β is not in effect small. The initial distribution for $\bar{u}$ was taken to be

$$\bar{u} = u_B + A_1\left\{\sum_1^\infty u_0^*(\bar{y})\cos n\beta Z\right\}, \tag{3.6a}$$

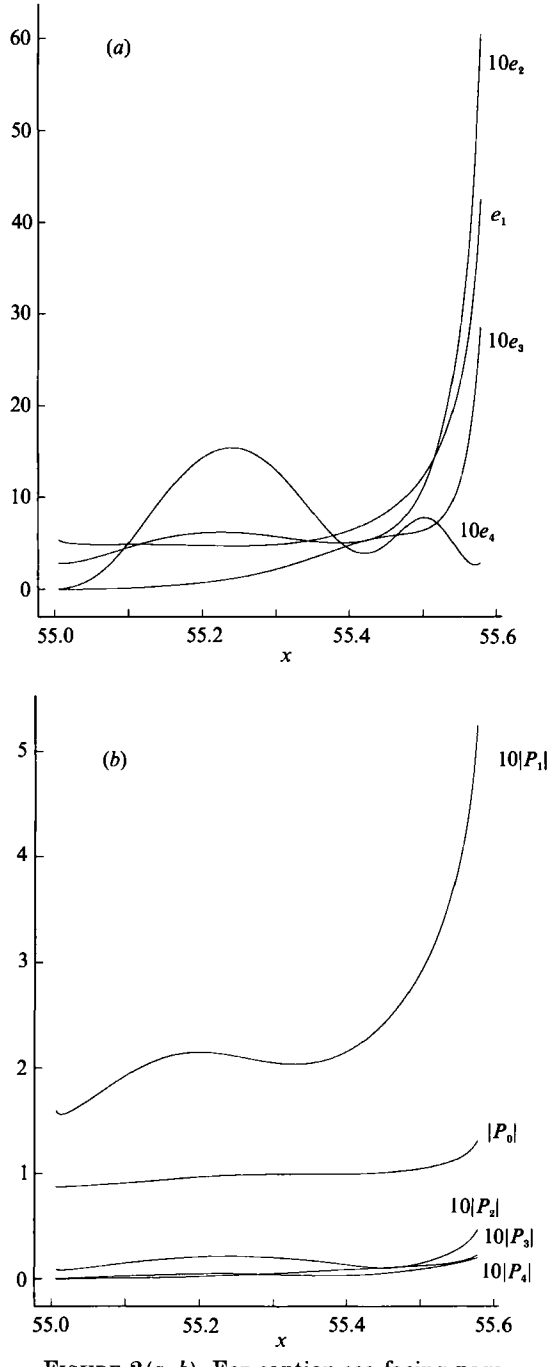

FIGURE 2(a, b). For caption see facing page.

where u_B is the Blasius profile, $u_0^* = e^{-\bar{y}} - e^{-2\bar{y}}$ and Δ_1 is parameter which can be varied so as to alter the size of the incoming vortex. The spanwise velocity $\bar{w}$ was then taken to be

$$\bar{w} = \sum_1^\infty \chi_n w_0^*(\bar{y}) \sin n\beta z, \tag{3.6b}$$

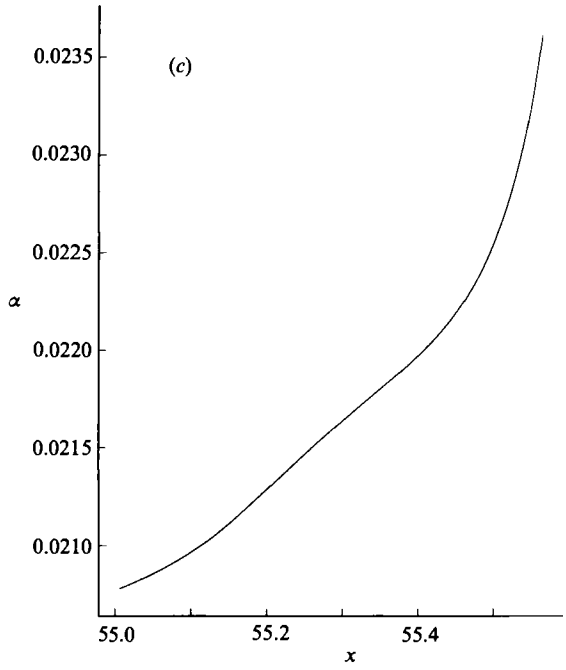

FIGURE 2. The development of (*a*) e_1, e_2, e_3, e_4, (*b*) P_0, P_1, P_2, P_3, P_4, and (*c*) α with x, for the case $\Delta_1 = 0.02$, $P_0 + \sum_1^\infty P_n = 1$ at $x = 55$.

with $w_0^* = \cos\bar{y}\,\mathrm{e}^{-\bar{y}}$ and χ_n chosen so that $\bar{w}$ satisfies the boundary condition on $\bar{w}$ at $\bar{y} = 0$ determined in terms of the Tollmien–Schlichting pressure. Clearly the above initial conditions are rather arbitrary but this is always the case with longitudinal vortex calculations unless the receptivity problem is discussed; see Hall (1983, 1989). Some limited experimentation with other initial conditions produced qualitatively similar results but we do not claim to have made an exhaustive investigation of the effects of the initial conditions on the vortex/wave interactions.

In order to monitor the evolution of the vortex and the wave, the following quantities were calculated as the flow was allowed to develop:

$$e_n = \int_0^\infty (\bar{u}_n^2 + \bar{w}_n^2)\,\mathrm{d}\bar{y}, \quad n = 1, 2, \ldots \tag{3.7a}$$

and P_n, where

$$P = P_0 + \sum_1^\infty P_n \cos n\beta Z. \tag{3.7b}$$

In figure 2 we show results from a calculation where the initial wave is almost two-dimensional. Figures 2(*a*), (*b*) show the development of e_1, e_2, e_3, e_4 and $P_0, P_1, \ldots, P_4$ respectively. Figure 2(*c*) shows the corresponding development of α. The calculations were started from $x = 55$ with $P_0 + \sum_1^\infty P_n = 1$ and $\Delta_1 = 0.02$. We see that the wave becomes progressively more three-dimensional as it moves downstream and that at a finite value x a singularity appears to arise, beyond which the solution cannot be calculated. The apparent singularity occurred in the same place when the finite-difference resolution was increased or the spectral resolution decreased. It was not possible for us to perform the calculations with more than eight Fourier modes because of our limited computing resources. However, we believe that figure 2

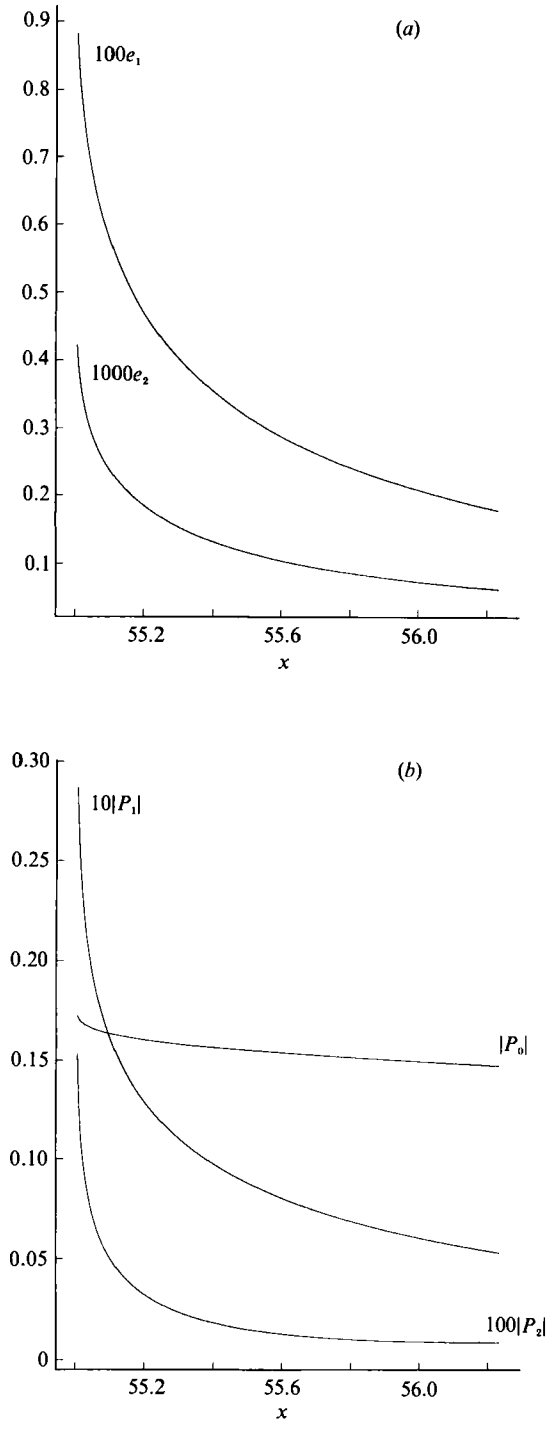

FIGURE 3. The development of (*a*) e_1, e_2 and (*b*) P_0, P_1, P_2 with x for the case $\Delta_1 = 0.02$, $P_0 + \Sigma_1^\infty P_n = 0.2$ at $x = 55$.

represents a significant calculation because it demonstrates the three-dimensional secondary instability, then nonlinearity and ultimate breakdown, of an initially two-dimensional wave and the induced vorticity structure. The resolution of the calculations was not great enough to determine whether the singularity encountered numerically is related to the ones discussed earlier in this section.

In figure 3 we show the results of a similar calculation but with smaller initial strengths for the vortex and wave fields. Here the vortex and waves decay as x increases. We note that the wave appears to effectively disappear before the vortex field. This is consistent with there being a subcritical bifurcation of a three-dimensional wave from a longitudinal vortex velocity field at a finite value of x (see our earlier comment concerning a square-root wave-pressure behaviour).

4. Nonlinear vortex/Rayleigh-wave interactions

Nonlinear interactions between longitudinal vortex flow and inviscid Rayleigh waves are considered here for the compressible or incompressible boundary layer, with, as a result, the boundary layer's $O(1)$ mean-flow profile again being changed completely from its original form.

The scales involved may be deduced mostly from a first-principles argument. Thus if the induced Rayleigh wave has pressure amplitude $\bar{\pi}$, its typical velocity amplitudes are also of order $\bar{\pi}$, by its inviscid nature, and the representative wavelengths are all of the short-scale size $Re^{-\frac{1}{2}}$. Hence the nonlinear inertial effect provoking a mean-flow correction is of order $\bar{\pi}^2 Re^{\frac{1}{2}}$, e.g. from uu_x, uv_x, uw_x. This is to be compared with the minimum inertial force in the typical long-scale vortex motion, namely $Re^{-\frac{1}{2}}$, for a full 'square' vortex of size as in (2.6a); this force is from the spanwise and normal momentum of the vortex, e.g. uv_x, uw_x (and the viscous forces such as $Re^{-1}w_{\bar{y}\bar{y}}$), rather than the strong streamwise momentum force of order unity. So the wave affects the mean flow at zeroth order if $\bar{\pi}^2 Re^{\frac{1}{2}}$ is comparable with $Re^{-\frac{1}{2}}$, i.e. if the wave pressure has amplitude $\bar{\pi} \sim Re^{-\frac{1}{2}}$ (smaller than in §2), in principle. There is a complication, however, similar to that in the vortex/TS case, namely the appearance of logarithmic behaviour in the induced vortex velocities close to the (linear) critical layer(s), situated at $\bar{y} = f$ say. The logarithmic response arises because the three-dimensional wave velocities there grow like $(\bar{y}-f)^{-1}$ (see below), so that the nonlinear inertial spanwise forcing is proportional to $(\bar{y}-f)^{-2}$, which can be balanced only by the viscous term $w_{\bar{y}\bar{y}}$ of the vortex with w proportional to $\ln|\bar{y}-f|$. Hence logarithmic contributions are drawn into play again, slightly altering the interactive balances.

In consequence the flow solution in the nonlinear vortex/compressible-Rayleigh-wave interaction (see also figure 1) has the underlying form

$$[u, v, w, p, \rho, T, \mu] = [\bar{u}, Re^{-\frac{1}{2}}\bar{v}, Re^{-\frac{1}{2}}\bar{w}, \bar{p}(x) + Re^{-1}\bar{p}_2, \bar{\rho}, \bar{T}, \bar{\mu}] + Re^{-\frac{1}{2}}[u^{(1)}, v^{(1)}, w^{(1)}, p^{(1)}, \rho^{(1)}, T^{(1)}, \mu^{(1)}]\mathscr{L}_1 + \ldots, \quad (4.1)$$

where the first square brackets on the right-hand side describe the mean flow or vortex motion, dependent only on the slower streamwise variable (x), and the second the wave, dependent on the faster streamwise variable (X), while $\mathscr{L}_1 = (\frac{1}{6}\ln Re)^{-\frac{1}{2}}$ is small. Along with this, multiple scaling of the form

$$\partial_x \to Re^{\frac{1}{2}}\partial_X + \partial_x$$

holds, in the spatial case here, with $x = Re^{-\frac{1}{2}}X$. Again, as in §2, the mean flow is to adjust to maintain the neutrality of the wave part here as distinct from growing

modes which would tend to produce nonlinearly an Euler stage as mentioned in §1 (and see later). The expansion (4.1) applies across most of the boundary layer, with $\bar{y}, \bar{z} \sim 1$, and leads to the compressible *vortex* equations

$$(\bar{\rho}\,\bar{u})_x + (\bar{\rho}\,\bar{v})_{\bar{y}} + (\bar{\rho}\,\bar{w})_{\bar{z}} = 0, \tag{4.2a}$$

$$\bar{\rho}(\bar{u}\,\bar{u}_x + \bar{v}\,\bar{u}_{\bar{y}} + \bar{w}\,\bar{u}_{\bar{z}}) = -\bar{p}'(x)/\gamma M_\infty^2 + (\bar{\mu}\,\bar{u}_{\bar{y}})_{\bar{y}} + (\bar{\mu}\,\bar{u}_{\bar{z}})_{\bar{z}}, \tag{4.2b}$$

$$\bar{\rho}(\bar{u}\,\bar{v}_{\bar{x}} + \bar{v}\,\bar{v}_{\bar{y}} + \bar{w}\,\bar{v}_{\bar{z}}) = -p_{2\bar{y}} + (\bar{\mu}\,\bar{u}_{\bar{y}})_x + (2\bar{\mu}\,\bar{v}_{\bar{y}})_{\bar{y}} + (\bar{\mu}(\bar{w}_{\bar{y}} + \bar{v}_{\bar{z}}))_{\bar{z}}, \tag{4.2c}$$

$$\bar{\rho}(\bar{u}\,\bar{w}_x + \bar{v}\,\bar{w}_{\bar{y}} + \bar{w}\,\bar{w}_z) = -p_{2\bar{z}} + (\bar{\mu}\,\bar{u}_{\bar{z}})_x + (\bar{\mu}(\bar{w}_{\bar{y}} + \bar{v}_{\bar{z}}))_{\bar{y}} + (2\bar{\mu}\,\bar{w}_{\bar{z}})_{\bar{z}}, \tag{4.2d}$$

$$\bar{\rho}\bar{T} = \bar{p}, \quad \bar{\mu} = C\bar{T}, \tag{4.2e,f}$$

$$\bar{\rho}(\bar{u}\,\bar{T}_x + \bar{v}\,\bar{T}_{\bar{y}} + \bar{w}\,\bar{T}_{\bar{z}}) = \sigma^{-1}\{(\bar{\mu}\,\bar{T}_{\bar{y}})_{\bar{y}} + (\bar{\mu}\,\bar{T}_{\bar{z}})_{\bar{z}}\} + (\gamma-1)\,\gamma^{-1}\bar{u}\,\bar{p}'(x) + (\gamma-1)\,M_\infty^2\,\bar{\mu}(\bar{u}_{\bar{y}}^2 + \bar{u}_{\bar{z}}^2), \tag{4.2g}$$

with

$$\bar{u} = \bar{v} = \bar{w} = 0, \quad \bar{T} = T_w \quad \text{at} \quad \bar{y} = 0, \tag{4.2h}$$

$$\bar{u} \to u_e(x), \quad \bar{T} \to T_e(x), \quad \bar{\rho} \to \rho_e(x), \quad \bar{w} \to 0 \quad \text{as} \quad \bar{y} \to \infty; \tag{4.2i}$$

and to the compressible Rayleigh equation for the effective *wave* pressure $\tilde{p}$,

$$\tilde{p}_{\bar{y}\bar{y}} + \tilde{p}_{\bar{z}\bar{z}} - \frac{2}{\bar{M}}(\bar{M}_{\bar{y}}\,\tilde{p}_{\bar{y}} + \bar{M}_{\bar{z}}\,\tilde{p}_{\bar{z}}) - \alpha^2(1-\bar{M}^2)\,\tilde{p} = 0 \tag{4.3a}$$

with

$$\tilde{p} \to 0 \text{ (or outgoing waves)} \quad \text{as} \quad \bar{y} \to \infty, \quad \tilde{p}_{\bar{y}} = 0 \quad \text{at} \quad \bar{y} = 0. \tag{4.3b,c}$$

Here the wave has $p^{(1)} = \tilde{p}\exp(\mathrm{i}\alpha X - \mathrm{i}\Omega\tilde{t}) + \text{c.c.}$, with $\alpha, \Omega (= \alpha c)$ real, the amplitude $\tilde{p}$ is independent of the faster scales $X, \tilde{t} = Re^{\frac{1}{2}}t$, and similarly for $u^{(1)}, v^{(1)}$, etc., leading to the inviscid response in (4.3). Also, $\bar{p}' = -\gamma M_\infty^2 \rho_e u_e u_e'$ is the external pressure gradient, $T_e(x), \rho_e(x)$ are the external temperature and density respectively, and $p_2 = \bar{p}_2/\gamma M_\infty^2 - (\bar{\mu}' - \frac{2}{3}\bar{\mu})(\bar{u}_x + \bar{v}_{\bar{y}} + \bar{w}_{\bar{z}})$, although we have in mind here mainly the case of the uniform stream with $\bar{p} \equiv 1$. The *nonlinear interaction* occurs through the definition of $\bar{M}$ required for (4.3),

$$\bar{M} = (\bar{u} - c)\,\bar{\rho}^{\frac{1}{2}} M_\infty, \tag{4.4a}$$

and through the boundary conditions on the vortex flow at the critical layer,

$$\bar{q} = -\frac{\gamma^{-2}\bar{\mu}^{-1}\Delta^{-\frac{3}{2}}}{M_\infty^2(\bar{M}')^2\alpha^2}\{\alpha^2\,\partial_{\bar{z}}(|\tilde{p}|^2) + \partial_{\bar{z}}(\Delta^{-1}|\tilde{p}_{\bar{z}}|^2)\} \tag{4.4b}$$

at

$$\bar{y} = f(x,\bar{z}) \pm \quad (\text{where } \bar{u} = c). \tag{4.4c}$$

Here $\bar{q}$ is the cross-flow velocity tangential to the critical-layer curve $\bar{y} = f(x,\bar{z})$, so that

$$\bar{q} = \Delta^{\frac{1}{2}}\bar{w}, \quad \bar{v} = f_{\bar{z}}\,\bar{w} \quad \text{at} \quad \bar{y} = f, \tag{4.4d}$$

and $\Delta = 1 + f_{\bar{z}}^2$; see also the next-but-one paragraph. The contribution (4.4*a*) describes the vortex-forcing of the wave, in essence, while the cross-flow slip velocity (4.4*b*) represents the main back-effect of the wave on the vortex motion, thus producing nonlinear interaction in which both the mean flow and the wave are unknown.

The main details behind the slip condition (4.4*b*) are presented in Appendix B, given the behaviour in (4.5)–(4.8) below.

The nonlinear vortex/Rayleigh-wave interaction is given by (4.2)–(4.4), for the compressible boundary layer. The pure spatial-development case is shown above, that for pure temporal development having $\bar{u}\,\bar{u}_x$ replaced by $\bar{u}_t$, etc., and a fixed

surface temperature is assumed as an example. Some of the comments in §2 apply here as well, and further points about the flow structure are the following. First, the induced slip velocity in (4.4*b*) clearly has a connection with that for TS waves in §2 corresponding to $f = 0$ and the high-frequency regime (see also §6). The tangential-flow condition on $(\bar{v}, \bar{w})$, incidentally, seems different from a usual vortex-sheet condition, since $\bar{u}f_x$ is absent. The present condition stems from the forcing terms on $\bar{v}, \bar{w}$ from Reynolds-stress-like contributions, denoted $\langle\ \rangle$ in Appendix B. We observe also, however, that the $\bar{q}$-term concerns the wave-forcing effects only and is additional to other contributions to $\bar{v}, \bar{w}$ which may come from the vortex evolution itself. Second, the relatively thin critical layer surrounding $\bar{y} = f$ is of the linear viscous kind, because the wave pressure amplitude $\bar{\pi}$ is only $O(Re^{-\frac{1}{2}}\mathscr{L}_1)$ (see references), and the thickness is of order $Re^{-\frac{2}{3}}$. From (4.3*a*), (4.4*a*), the wave response nearby as $\bar{y} \to f\pm$ is of the form

$$\tilde{p} \sim \tilde{p}_0 + s\tilde{p}_1 + s^2\tilde{p}_2 + s^3\tilde{p}_3 + \ldots, \tag{4.5a}$$

where $s = \bar{y} - f$, in general logarithmic terms must be absent to allow both α and c to remain real, and

$$\bar{M} \sim s\bar{M}_1 + s^2\bar{M}_2 + \ldots, \tag{4.5b}$$

with the coefficients above being z-dependent and related by

$$\tilde{p}_1 \Delta = \tilde{p}_{0\bar{z}} f_{\bar{z}}, \tag{4.6a}$$

$$-2\tilde{p}_2 \Delta - f_{\bar{z}\bar{z}}\tilde{p}_1 + 2\bar{M}_{1\bar{z}}(f_{\bar{z}}\tilde{p}_1 - \tilde{p}_{0\bar{z}})/\bar{M}_1 + \tilde{p}_{0\bar{z}\bar{z}} - \alpha^2\tilde{p}_0 = 0, \tag{4.6b}$$

$$\begin{aligned} &-2\tilde{p}_{2\bar{z}} f_{\bar{z}} - 2\tilde{p}_2(f_{\bar{z}\bar{z}} + 3\Delta\bar{M}_2/\bar{M}_1 - 2\bar{M}_{1\bar{z}} f_{\bar{z}}/\bar{M}_1) + \tilde{p}_{1\bar{z}\bar{z}} + 2(\bar{M}_2 f_{\bar{z}} - \bar{M}_{1\bar{z}})\tilde{p}_{1\bar{z}}/\bar{M}_1 \\ &+ \tilde{p}_1(-\alpha^2 + 2\bar{M}_{2\bar{z}} f_{\bar{z}}/\bar{M}_1 - \bar{M}_2 f_{\bar{z}\bar{z}}/\bar{M}_1) + [\bar{M}_2(\tilde{p}_{0\bar{z}\bar{z}} - \alpha^2\tilde{p}_0) - 2\bar{M}_{2\bar{z}}\tilde{p}_{0\bar{z}}]/\bar{M}_1 = 0. \end{aligned} \tag{4.6c}$$

(In principle these give three equations fixing the three terms $\tilde{p}_0$, $\tilde{p}_1$, $\tilde{p}_2$). Hence it follows that the three-dimensional wave velocities are given locally by

$$\tilde{u} \sim F_{-1}s^{-1} + F_0 + \ldots, \tag{4.7a}$$

$$\tilde{v} \sim G_{-1}s^{-1} + G_0 + \ldots, \tag{4.7b}$$

$$\tilde{w} \sim H_{-1}s^{-1} + H_0 + \ldots, \tag{4.7c}$$

as anticipated at the start of this section; in addition $\tilde{\rho} \sim -\bar{\rho}_{\bar{z}}\tilde{p}_{0\bar{z}}/(\gamma\alpha^2\bar{M}_1^2\Delta s^2)$. Here the inviscid disturbance equations show that

$$\gamma M_\infty^2 \bar{\rho}_0 G_{-1} = -\tilde{p}_1/\mathrm{i}\alpha\bar{u}_1, \tag{4.8a}$$

$$\gamma M_\infty^2 \bar{\rho}_0 H_{-1} = (f_{\bar{z}}\tilde{p}_1 - \tilde{p}_{0\bar{z}})/\mathrm{i}\alpha\bar{u}_1, \tag{4.8b}$$

$$\gamma M_\infty^2 \bar{\rho}_0 F_{-1} = -H_{-1\bar{z}}/\mathrm{i}\alpha, \tag{4.8c}$$

consistent with (4.6*a–c*), where $\bar{\rho} \sim \bar{\rho}_0 + \bar{\rho}_1 s + \ldots, \bar{u} - c \sim \bar{u}_1 s + \bar{u}_2 s^2 + \ldots$. See also Appendix C for the incompressible regime. The singular behaviour in (4.7*a–c*) is responsible for the generation, at the amplitude-squared level, of the logarithmic-flow effect which leads to the effective slip in (4.4*b*), via the $O(Re^{-\frac{3}{4}})$ critical layer (see Appendix B). Third, the three-dimensional-wave condition in (4.6*a–c*) can be shown to agree with the generalized inflexion-point condition for two- or three-dimensional simple waves on a parallel flow (and with other simpler cases), from consistency between (4.6*b*, *c*), requiring $\bar{M}_2 = 0$ in general, and with $\tilde{p}_1 = 0$ from (4.6*a*) then. The latter waves can act as triggering mechanisms for the present nonlinear interaction. Fourth, the continuity properties of the total mean flow $\bar{u}, \bar{v}, \bar{w}$ across the critical layer are worth noting. These are that $\bar{u}, \bar{u}', \bar{u}'', \bar{v}, \bar{v}', \bar{w}$ are all continuous, with

discontinuities appearing first in $\bar{u}''', \bar{v}'', \bar{w}'$ (the prime denotes the normal derivative), and requiring higher-order smoothing within the critical layer, which is addressed in Appendix B. Fifth, the wave's inertial effects on the mean flow are felt solely in the slip condition (4.4*b*) to leading order, the effects in the rest of the boundary layer being negligible (just!) owing to the logarithmic response described earlier.

5. Special cases and limit solutions

The vortex/compressible-Rayleigh-wave nonlinear interaction set up in §4 poses a computational task, in general, which seems a particularly severe one in view of the unknown moving boundary present (in (4.4)) and the coupled partial-differential systems (4.2), (4.3). No full solutions have been obtained yet, and appropriate computational treatments are only just being considered. For that reason we turn briefly here, in (i)–(vii) below, to certain special or limiting properties, to help provide some possible guidelines and suggestions.

(i) The linearized version, where $\bar{w}$ and ∂_z are identically zero in (4.2) and $\bar{u}, \bar{v}$ take on the compressible Blasius form, say, applies at small wave amplitudes $|\tilde{p}|$ and leaves the linear compressible-Rayleigh equation (4.3) controlling instability, with $\bar{M}$ known in advance. Solution properties at various Mach numbers are given by Mack (1975, 1984) and Malik (1982, 1987) principally. The main result in the present context is that neutral modes exist at all Mach numbers (see e.g. Mack's 1984 figures) and so can act as triggers for the nonlinear interaction of §4. See also (iv) below.

(ii) Weak nonlinearity can also be handled analytically in principle, an example being for two input oblique waves of lowish amplitudes. This is analogous to the Hall & Smith (1989) oblique-wave/vortex analysis in the TS case, and includes secondary three-dimensional instability at the start, as does the full system of §4.

(iii) Wide-vortex/wave interactions similar to those in §2 can arise as limit cases of (4.2)–(4.4) for enlarged spanwise scales.

(iv) Special ranges of the Mach number M_∞ are of theoretical and practical interest, including zero M_∞ (see also Appendix B), small M_∞, the transonic range $M_\infty \to 1$, and the hypersonic range of large M_∞. These have connections, in turn, with the vast literature on linear incompressible Rayleigh modes in boundary layers, with Gajjar's (1989) linear and nonlinear critical-layer work, with Bowles' (1989) linear and nonlinear instability work, and with recent studies of linear hypersonic-flow instabilities. Concerning the hypersonic range in particular, the undisturbed steady two-dimensional boundary layer with no imposed pressure gradient itself acquires a two-layered form at large Mach numbers (Bush 1966; Lee & Cheng 1969; Stewartson 1964), with a relatively wide high-temperature layer, wherein $\bar{y}$ is $O(M_\infty^2)$, at the upper edge of which is a relatively thin high-vorticity layer with $\bar{y} - M_\infty^2 F(x)$ of order $(\ln M_\infty^2)^{\frac{1}{2}}$. Here $\bar{y} = M_\infty^2 F(x)$ denotes the scaled boundary-layer displacement. In line with this, the linear instability modes split into two types, the so-called vorticity mode concentrated within the high-vorticity layer and having the maximum growth rate (Brown & Smith 1990), and the so-called acoustic modes which spread normally across the $O(M_\infty^2)$ layer and have smaller growth rates (Cowley & Hall 1990; Brown & Smith 1990). These linear features agree quite well with Mack's results at large M_∞ and suggest the two most likely structures of nonlinear vortex/compressible-Rayleigh interaction at large M_∞, as follows.

First, the high-vorticity form of nonlinear interaction occurs where

$$\bar{y} = M_\infty^2 F(x) + (2\Gamma)^{-1}\bar{y} \quad (\text{with} \quad \Gamma \exp(\Gamma^2) = M_\infty^2) \tag{5.1a}$$

and the scalings operating are of the form

$$\bar{u} = 1 - \bar{u}_1/M_\infty^2, \quad \bar{v} = M_\infty^2 F_x \bar{u} + 2\Gamma\bar{V}, \quad \bar{w} = M_\infty \bar{W}/(2\Gamma)^{\frac{1}{2}}, \tag{5.1b}$$

$$\bar{z} = M_\infty (2\Gamma)^{-\frac{5}{2}} \hat{z}, \tag{5.1c}$$

$$\bar{\rho} \sim 1, \quad \bar{T} \sim 1, \quad \bar{\mu} \sim 1. \tag{5.1d}$$

These scalings are implied by the Prandtl shift in $\bar{y}$, in (5.1a), which introduces in effect a large Görtler number $M_\infty^2 F_{xx}$ (for the high-vorticity-layer flow) that is negative for flat-surface flow where $F \propto +x^{\frac{1}{2}}$. Thus the vortex becomes relatively 'wide'. It is also quasi-two-dimensional in the cross-flow plane, since its governing equations become

$$(\bar{\rho}\bar{V})_{\hat{y}} + (\bar{\rho}\bar{W})_{\hat{z}} = 0, \tag{5.2a}$$

$$\bar{\rho} F_{xx} = -\hat{\pi}_{\hat{y}} \tag{5.2b}$$

$$\bar{\rho}(\bar{V}\bar{W}_{\hat{y}} + \bar{W}\bar{W}_{\hat{z}}) = -\hat{\pi}_{\hat{z}} + (\bar{\mu}\bar{W}_{\hat{y}})_{\hat{y}}, \tag{5.2c}$$

$$\bar{\rho}(\bar{V}\bar{T}_{\hat{y}} + \bar{W}\bar{T}_{\hat{z}}) = \sigma^{-1}(\bar{\mu}\bar{T}_{\hat{y}})_{\hat{y}}, \tag{5.2d}$$

$$\bar{\rho}\bar{T} = 1, \quad \bar{\mu} = C\bar{T}, \tag{5.2e,f}$$

$$\bar{\rho}(\bar{V}\bar{u}_{1\hat{y}} + \bar{W}\bar{u}_{1\hat{z}}) = (\bar{\mu}\bar{u}_{1\hat{y}})_{\hat{y}}, \tag{5.2g}$$

from (4.2) with (5.1). The coupled wave-amplitude equation, however, is now

$$\hat{p}_{\hat{y}\hat{y}} - 2(\hat{M}_{\hat{y}}/\hat{M})\hat{p}_{\hat{y}} - \hat{\alpha}^2\hat{p} = 0, \tag{5.3a}$$

where

$$\hat{M} \equiv (c_1 - \bar{u}_1)\bar{\rho}^{\frac{1}{2}}, \tag{5.3b}$$

upon suitable scaling in (4.3); and the back reaction of the wave on the vortex motion is felt through the slip condition

$$\bar{W} = -\frac{1}{3C\gamma^2(\bar{u}_1'(\hat{y}_c))^2}\partial_{\hat{z}}(|\hat{p}|^2) \tag{5.4}$$

at the unknown critical-level curve, from (4.4). Hence, despite the quasi-planar balances in (5.2*a–f*), the streamwise momentum balance (5.2*g*) in the vortex still exerts influence on the nonlinear interaction owing to the appearance of $\bar{u}_1$ in (5.3*b*) and (5.4). We observe that an alternative type of nonlinear interaction can arise either with sufficient surface curvature present, if the resulting Görtler number is equal to $M_\infty^2 F_{xx} + O(\Gamma^{-1})$, or with negligible curvature F_{xx}, since then the vortex can remain 'square', more like those in §4 and below. Again, for small wave amplitudes linearized properties hold, with (5.2), (5.4) reproducing the basic boundary-layer solution via the Howarth–Dorodnitsyn transformation, while (5.3) then gives the equation addressed by Brown & Smith (1990) for which the neutral wavenumber is $\hat{\alpha} = \frac{1}{4}$. Comments similar to those in (i), (ii) above apply thereafter. There is also a neat, exact, local solution to the full system (5.2)–(5.4), described in Walton (1991), and a possible link with the experimental studies of Holden (1985), where pronounced rope-like vortex motions were observed at the edges of hypersonic boundary layers in the Mach-number range 11–13.

The second of the large-M_∞ interaction structures is rather simpler, its scales being implied by the $O(M_\infty^2)$ thick boundary-layer form. Thus here

$$(\bar{y}, \bar{z}, \bar{T}, \bar{v}, \bar{w}, p_2) \sim M_\infty^2, \tag{5.2a}$$

$$\bar{u} = O(1), \quad (\bar{\rho}, \alpha) \sim M_\infty^{-2}, \quad \tilde{p} \sim M_\infty^4, \tag{5.5b}$$

leaving the complete nonlinear interaction system (4.2)–(4.4) essentially intact. The only new feature here is that the boundary-layer's normal extent becomes finite, $0 \leqslant \bar{y} < \bar{F}$ say, in normalized terms. The linearized version then matches up with the linear acoustic-modes analyses of Hall & Cowley and Brown & Smith, after which comments as in (i), (ii) again apply. It may be significant however that there are

infinitely many acoustic modes, and hence possible bifurcations, available usually as the flow proceeds downstream, in contrast with the single vorticity mode; and the modes present with large wavenumbers, as well as mode-crossing (Brown & Smith), may shed extra light on the nonlinear interaction process.

(v) Extreme surface conditions, values of the parameters present such as σ, C, or pressure gradients, could also provide extra insight.

(vi) Besides the many applications within boundary-layer transition summarized above, and the corresponding computational tasks, and nonlinear similarity forms for instance, there are also many other flow configurations to which vortex/Rayleigh-wave interaction applies in principal (see §6 and Appendix C).

(vii) Finally here, we should mention the possibility that the Smith & Walton (1989) breakdown summarized in (3.2) also describes the ultimate behaviour of the present vortex/compressible-Rayleigh nonlinear systems, at least for wide vortices. If so, the boundary layer again separates, effectively, splitting into two increasingly far-apart layers, with only slow motion in-between, at a finite distance downstream. That opens up an intriguing prospect, namely that a vortex/wave interaction (either as in §2 or as in §4) can induce separation (as above), which then introduces an extra (inflexional) inviscid mode and then an extra vortex/wave nonlinear interaction, which leads to another separation, hence another interaction, and so on. This self-generating process causes the whole flow structure locally to cascade into smaller lengthscales, and thence into substructures.

6. Further comments

The present work extends our previous studies of vortex/wave interaction (Hall & Smith 1988, 1989, 1990) to the strongly nonlinear regime in which the entire mean-flow profile, at any station x, is altered substantially from its undisturbed laminar form. This is for the compressible boundary-layer setting in the nonlinear vortex/Rayleigh interaction of §4 (the incompressible version is noted in Appendix C) and for the incompressible case in the nonlinear vortex/TS interaction of §2, with the corresponding compressible vortex/TS interaction following readily from a combination of those two sections (see also Smith & Walton 1989) and below. The solution properties and suggestions given in §§3 and 5 hint fairly strongly, we believe, at the potential power of these nonlinear interactions in terms of full transition of the flow. In addition, it appears that numerous waves can be triggered (see §5), all interacting nonlinearly with the unknown mean flow, especially if separation is approached for instance. These and other features of the nonlinear interactions found seem to offer exciting prospects for more complete theoretical understanding of fully fledged boundary-layer transition.

Some numerical work for fully nonlinear interaction is described in §3, for the vortex/TS case, but further concerted efforts on full computations, for both the vortex/TS and the vortex/Rayleigh cases, are undoubtedly necessary and these represent a major challenge. They should enable quantitative comparisons with experiments and direct numerical simulations to be made eventually (an encouraging point being that qualitatively the flow structures in §§2 and 4 seem to be in line with the numerical-simulation experience, e.g. of Kleiser, that many more spanwise than streamwise wavenumbers are required to accurately describe fully fledged transition, except in its later stages.) The pure spatial problem, the pure temporal problem, and the combined problem featuring the operator $\partial_t + \bar{u}\partial_x$ are all of interest here since they might provoke different ultimate behaviour and hence possibly different views

of such phenomena as lambda-vortex formations (suggested by Smith & Walton 1989) and the successive collapses in scales referred to in §§3 and 5. The latter in turn may lead on to the three-dimensional Euler stage locally, cf. Smith (1988), Hoyle *et al.* (1991), Peridier, Smith & Walker (1991*a*, *b*) for nonlinear TS transition, allowing comparisons with experiments and direct numerical simulations (e.g. those of Zang, Erlebacher, Hussaini, Kleiser and Biringen) on the later stages of transition, including spikes, intermittency and streak production. In all this, however, the computational tasks set by the nonlinear interaction problems posed in §2 and in (4.2)–(4.4) for instance seem to present a main hurdle.

Certain other interesting aspects of the vortex/wave interactions should also be put on record here. These are: various limiting or simplified cases, such as those in §5; similarity solutions (cf. §3; Walton 1991); the analogy with Görtler-vortex development (based on Hall 1982, 1983 and subsequent works); non-equilibrium critical-layer effects (in the context of §4); high-frequency properties (for §§2 and 4); and the implications for by-pass transition where the nonlinear interactions do not start from linear small-disturbance growth.

The nonlinear vortex/wave interactions also have numerous potential applications for other types of flows, in all of which the essential ideas of §2 and/or §4 would seem to apply: in wakes, channel flows (Bennett *et al.* 1991), pipe flows (Walton 1991), plane Couette flow, water motions, free shear layers, separations, vortex breakdown, where a swirl-velocity component is added to the vortex motion (and separation such as in (3.2) could correspond to abrupt vortex thickening), and flows over surface roughnesses, for example. See also Appendix C. The ideas apply further to lengthscales other than those taken in §§2 and 4. Again, there may be extensions of interest along the following lines: upper-branch flow structures, connected with the high-frequency TS limit; non-Chapman fluids and real-gas effects; surface-cooling effects (Seddougui, Smith & Bowles 1991; external-shock interactions in hypersonic flow, where the acoustic modes (§5) could play an important part; external pressure-gradient influences; and alternative compressible interactions. Nevertheless, the major pressing challenge seems to us to be the computational one of accurately solving the vortex/wave nonlinear interaction equations set up in §§2 and 4, given the encouraging guidelines on the strongly nonlinear effects possible.

Interesting and helpful comments were made by three referees, and by Miss P. G. Brown, Mr D. A. Davis and Dr J. W. Elliott who also kindly pointed out a number of corrections. An earlier version of this work appeared as our 1989 ICASE Report No. 89–82. The authors wish to acknowledge ICASE, SERC and AFOSR (grant no. 89-0475) who supported parts of this work.

Appendix A. More details behind the vortex/Tollmien–Schlichting interaction equations

For the wide-vortex/TS interaction of (2.2)–(2.4) the triple-deck structure holds, as with most TS linear or nonlinear interactions. Near the surface, in the lower deck containing the viscous critical layer, the total velocity and pressure are given by

$$u = Re^{-\frac{1}{8}}\bar{\lambda}Y + Re^{-\frac{1}{4}}\hat{\mathscr{L}}(\hat{u}_1 E + \text{c.c.}) + \ldots + Re^{-\frac{3}{8}}\hat{\mathscr{L}}^2\bar{u}_{\text{v}} + \ldots \tag{A 1}$$

$$v = Re^{-\frac{1}{2}}\hat{\mathscr{L}}(\hat{v}_1 E + \text{c.c.} + \ldots + Re^{-\frac{5}{8}}\hat{\mathscr{L}}^2\bar{v} + \ldots, \tag{A 2}$$

$$w = Re^{-\frac{1}{4}}\hat{\mathscr{L}}(\hat{w}_1 E + \text{c.c.}) + \ldots + Re^{-\frac{3}{8}}\hat{\mathscr{L}}^2\bar{w}_{\text{v}} + \ldots, \tag{A 3}$$

$$p = Re^{-\frac{3}{8}}\hat{\mathscr{L}}(PE + \text{c.c.}) + \ldots, \tag{A 4}$$

in effect. Here the mean-flow skin-friction factor $\bar{\lambda}(x, Z)$ is defined in (2.3*b*), $y = Re^{-\frac{5}{8}}Y$, and $PE + \text{c.c.}$ is equal to P_1 in (2.1*d*). Substitution into the Navier–Stokes equations leads, first, to the unsteady linearized three-dimensional boundary-layer equations for the wave part, as a small perturbation of the unknown shear flow $u = Re^{-\frac{1}{8}}\bar{\lambda}Y$, so that

$$\mathrm{i}\alpha\hat{u}_1 + \hat{v}_{1Y} + \hat{w}_{1Z} = 0, \tag{A 5}$$

$$(-\mathrm{i}\Omega + \mathrm{i}\alpha\bar{\lambda}Y)\,\hat{u}_1 + \hat{v}_1\bar{\lambda} + \hat{w}_1\bar{\lambda}_Z = -\mathrm{i}\alpha P + \hat{u}_{1YY}, \tag{A 6}$$

$$(-\mathrm{i}\Omega + \mathrm{i}\alpha\bar{\lambda}Y)\,\hat{w}_1 = -P_Z + \hat{w}_{1YY}, \tag{A 7}$$

from the balances of continuity, x-momentum and z-momentum in turn. The y-momentum balance confirms that P is independent of Y. The solution of the governing equations (A 5)–(A 7) together with the appropriate boundary conditions (no slip at $Y = 0$, and $\hat{u}_1 \to A$, $\hat{w}_1 \to 0$ as $Y \to \infty$) then yields the TS pressure equation (2.3*a*), after some working as in Smith (1979*b*), involving the effective negative displacement A of the wave and the Airy-related functions shown in (2.5*a–d*).

At second order, the amplitude-squared forcing from the wave parts produces a mean- or vortex-flow contribution $\propto E^0$, among others, since α, Ω are real. The controlling equations here, again from substitution of (A 1)–(A 4) into the Navier–Stokes equations, have a form analogous to those in (B 10), (B 12) in Appendix B, for the vortex part $\bar{u}_{\mathrm{v}}, \bar{w}_{\mathrm{v}}$, with the notation suitable changed (and $f \equiv 0$ now). The forcing terms $\langle\,\rangle$ in the z-momentum vortex balance decay as Y^{-2} at large Y, however, since $\hat{w}_1$ and $\hat{u}_1 - A$ decay algebraically $\propto Y^{-1}$, from the solution of (A 5)–(A 7), as $Y \to \infty$. Hence the viscous term $\partial^2\bar{w}_{\mathrm{v}}/\partial Y^2$ in the z-momentum vortex balance leads to the logarithmic growth

$$\bar{w}_{\mathrm{v}} \sim -\bar{\lambda}_{\mathrm{v}}^{-2}\partial_Z[|P|^2 + \alpha^{-2}|P_Z|^2]\ln Y \quad \text{as} \quad Y \to \infty \tag{A 8}$$

of the spanwise velocity of the vortex motion. The behaviour (A 8) therefore implies the inner constraint (2.2*d*) on $\bar{w}$, or the spanwise slip velocity, as observed in the main deck where $Y \to Re^{\frac{1}{8}}\bar{y}$ effectively, as well as the scaling factor $\hat{\mathscr{L}}$ in (2.1*b*).

In the main deck, the majority of the boundary layer, the flow solution expands in the (displaced-flow) form

$$u = \bar{u}(x, \bar{y}, Z) + Re^{-\frac{1}{4}}\hat{\mathscr{L}}(AE\bar{u}_{\bar{y}} + \text{c.c.}) + \ldots \tag{A 9}$$

effectively, and so on, as inferred from the expansions (2.1*a*, *c*) added together, and matching with (A 1)–(A 4). Here the Navier–Stokes equations are satisfied to the required order provided that the vortex equations (2.2*a–c*) hold.

The expansion in the upper deck just outside the boundary layer then takes the form

$$u = u_{\mathrm{e}}(x) + Re^{-\frac{3}{8}}\hat{\mathscr{L}}(u_1 E + \text{c.c.}) + \ldots, \tag{A 10}$$

$$p = Re^{-\frac{3}{8}}\hat{\mathscr{L}}(\tilde{p}E + \text{c.c.}) + \ldots, \tag{A 11}$$

and so on, such that in (2.1*b*) $\tilde{p}_1 = \tilde{p}E + \text{c.c.}$ There is therefore a small perturbation of the free stream in effect, giving potential-flow equations, for example, with $\mathrm{i}\alpha u_1 + \partial v_1/\partial\tilde{y} + \partial w_1/\partial Z = 0$ for continuity, where $y = Re^{-\frac{3}{8}}\tilde{y}$ in the upper-deck scaling. These potential-flow equations along with the required matching conditions give the wave response summarized in (2.4*a–c*). The feedback pressure effect on the main vortex part, from the upper-deck motion, remains negligible at the present order.

Virtually all the above features come directly from §6 of Smith & Walton (1989),

when h there is replaced by $Re^{-\frac{1}{8}}$. For our §4, a similar exercise of substitution (of the expansions (4.1)) into the Navier–Stokes equations leads to the governing equations (4.2)–(4.4).

Appendix B. The critical-layer behaviour (for vortex/Rayleigh-wave interactions)

The critical layer occurs when $y = Re^{-\frac{1}{8}} f(x,\bar{z}) + Re^{-\frac{3}{8}} Y$, with Y of $O(1)$, and the flow properties produced are predominantly linear. The solution takes the form

$$u = c + Re^{-\frac{1}{8}}\lambda_1(x,\bar{z})\,Y + \ldots + Re^{-\frac{1}{2}}\mathscr{L}_1 U^{(1)} + \ldots + Re^{-\frac{1}{2}}(\mathscr{L}_1^2\bar{U} + \mathscr{L}_1 U^{(2)}) + \ldots, \quad \text{(B 1)}$$

$$v = \ldots + Re^{-\frac{1}{8}}\mathscr{L}_1 V^{(1)} + Re^{-\frac{1}{2}}(\mathscr{L}_1^2 f_{\bar{z}}\bar{W} + \mathscr{L}_1 V^{(2)} + f_{\bar{z}}\bar{W}_M) + \ldots + Re^{-\frac{3}{8}}(\mathscr{L}_1^2\bar{V} + f_{\bar{z}}\bar{W}_N + \bar{V}_M) + \ldots, \quad \text{(B 2)}$$

$$w = \ldots + Re^{-\frac{1}{8}}\mathscr{L}_1 W^{(1)} + \ldots + Re^{-\frac{1}{2}}(\mathscr{L}_1^2\bar{W} + \mathscr{L}_1 W^{(2)} + \bar{W}_M) + \ldots + Re^{-\frac{3}{8}}\bar{W}_N + \ldots, \quad \text{(B 3)}$$

$$p = \ldots + Re^{-\frac{1}{2}}\mathscr{L}_1 P^{(1)} + \ldots + Re^{-\frac{3}{8}}\mathscr{L}_1 P^{(2)} + \ldots, \quad \text{(B 4)}$$

where λ_1 is the streamwise vortex shear at the critical layer, the main wave part (superscript (1)) depends on the fast scales $(X,\tilde{t}) = Re^{\frac{1}{8}}(x,t)$ with wavespeed c as in §4, and the main vortex part (overbarred) is independent of the fast scales. Here we discuss the incompressible case with zero pressure gradient, for the sake of clarity; the compressible version follows along similar lines.

The successive balances in mass conservation resulting from (B 1)–(B 4) give

$$V_Y^{(1)} = f_{\bar{z}} W_Y^{(1)}, \quad \text{(B 5)}$$

$$U_X^{(1)} + V_Y^{(2)} + W_{\bar{z}}^{(1)} - f_{\bar{z}} W_Y^{(2)} = 0, \quad \text{(B 6)}$$

$$c_x - f_x\lambda_1 + \bar{V}_{MY} + \bar{W}_{M\bar{z}} = 0, \quad \text{(B 7)}$$

and the x-momentum balances of concern are

$$V^{(1)} = f_{\bar{z}} W^{(1)}, \quad \text{(B 8)}$$

$$\lambda_1 Y U_X^{(1)} + \lambda_1 V^{(2)} + W^{(1)}\lambda_{1\bar{z}} Y - W^{(2)} f_{\bar{z}}\lambda_1 = -P_X^{(1)} + \Delta U_{YY}^{(1)}, \quad \text{(B 9)}$$

$$\langle U^{(1)}U_X^{(1)} + V^{(2)}U_Y^{(1)} + W^{(1)}U_{\bar{z}}^{(1)} - W^{(2)}f_{\bar{z}}U_Y^{(1)}\rangle + \bar{V}\lambda_1 + \bar{W}Y\lambda_{1\bar{z}} + \ldots = \ldots + \Delta\bar{U}_{YY}. \quad \text{(B 10)}$$

Likewise, the z-momentum balances here become

$$\lambda_1 Y W_X^{(1)} = -P_{\bar{z}}^{(1)} + f_{\bar{z}} P_Y^{(2)} + \Delta W_{YY}^{(1)}, \quad \text{(B 11)}$$

$$\langle U^{(1)}W_X^{(1)} + V^{(2)}W_Y^{(1)} + W^{(1)}W_{\bar{z}}^{(1)} - W^{(2)}f_{\bar{z}}W_Y^{(1)}\rangle \ldots = \ldots + \Delta\bar{W}_{YY}, \quad \text{(B 12)}$$

while the $y-$momentum equation implies that $P^{(1)}$ is independent of Y, and hence equal to $p^{(1)}$, and

$$P_Y^{(2)} = -\lambda_1 Y V_X^{(1)} + \Delta V_{YY}^{(1)}. \quad \text{(B 13)}$$

In (B 10), (B 12), $\langle\ \rangle$ refers to the vortex components only, in the enclosed terms.

The wave part in this non-flat critical layer may be analysed by putting $V^{(2)} - f_{\bar{z}}W^{(2)} = V_a$, say, which leaves $U^{(1)}$, V_a, $W^{(1)}$ satisfying essentially the equations of a linear three-dimensional disturbance in a standard flat critical layer, from (B 6), (B 9), (B 11), (B 13) and since $V^{(1)} = f_{\bar{z}}W^{(1)}$ from (B 5), (B 8). In particular, $W^{(1)}$ satisfies a forced Airy equation in the form

$$\lambda_1 Y W_X^{(1)} = -P_{\bar{z}}^{(1)}\Delta^{-1} + \Delta W_{YY}^{(1)}, \quad \text{(B 14)}$$

which yields the solution

$$W^{(1)} = -(\Delta^2\lambda_1 \mathrm{i}\alpha)^{-\frac{2}{3}}\tilde{p}_{\bar{z}}\mathscr{I}(\hat{Y})E + \text{c.c.}, \quad Y = (\Delta/\lambda_1 \mathrm{i}\alpha)^{\frac{1}{3}}\hat{Y}, \tag{B 15}$$

where $\mathscr{I}$ satisfies $\mathscr{I}'' - \hat{Y}\mathscr{I} = 1$, $\mathscr{I}(\pm\infty) = 0$, and can be expressed in terms of the Airy function, and $E = \exp(\mathrm{i}\alpha X - \mathrm{i}\Omega\tilde{t})$. This and the corresponding solutions for V_a, $U^{(1)}$ are smooth for all Y and satisfy the asymptotic conditions of matching,

$$[U^{(1)}, V^{(1)}, W^{(1)}] \sim Y^{-1}[F_{-1}, G_{-1}, H_{-1}]E + \text{c.c.},$$
$$[V^{(2)}, W^{(2)}] \to [G_0, H_0]E + \text{c.c.} \quad \text{as} \quad Y \to \pm\infty, \tag{B 16}$$

implied by (4.7), (4.8) (with Appendix C), as required.

Then the main vortex equation of interest here is that for $\bar{W}$, in (B 12). Here the behaviour in (B 16) shows that the nonlinear forcing term on the left-hand side of (B 12) decays as Y^{-2} as $Y \to \pm\infty$. So, with allowance made for the normal pressure variation due to the Y-momentum balance, double integration of (B 12) with respect to Y produces the response

$$\bar{W} \sim -\hat{B}\ln|Y| \quad \text{as} \quad Y \to \pm\infty, \tag{B 17}$$

with

$$\hat{B} = \Delta^{-1}[2(H_{-1}H^*_{-1})_{\bar{z}} + (f_{\bar{z}}H_0 - G_0)H^*_{-1} + (f_{\bar{z}}H^*_0 - G^*_0)H_{-1} + 2f_{\bar{z}}f_{\bar{z}\bar{z}}|H_{-1}|^2\Delta^{-1}]$$

being found to equal $-\bar{q}\Delta^{-\frac{1}{2}}$ as defined in (4.4*b*) or in Appendix C. The logarithmic behaviour in (B 17) and the associated logarithmic terms in $\bar{U}, \bar{V}$ at large $|Y|$ are responsible for the scale factor $\mathscr{L}_1$ in (4.1), as well as for the effective slip condition in (4.4*b*). The condition (4.4*b*) follows from the match with the flow solution in §4, since $\ln|Y| \to \frac{1}{6}\ln Re + \ln|\bar{y} - f|$ in effect.

Appendix C. Vortex/Rayleigh-wave interactions in the incompressible case

Many of the extra applications mentioned in the text are concerned more with incompressible fluids, for which the vortex/wave interaction equations (4.2)–(4.4) continue to hold provided $\bar{\rho}, \bar{\mu}$ are replaced by unity in (4.2*a–d*), $\bar{M}$ is replaced by $(\bar{u} - c)$ in (4.3*a*), with the $\bar{M}^2$ term omitted, and (4.4*b*) is replaced by

$$\bar{q} = -[\Delta^{-\frac{3}{2}}/(\bar{u}_1)^2\alpha^2]\{\}, \tag{C 1}$$

where the curly brackets signify the curly-bracketed expression in (4.4*b*). The governing equations in that case are (4.2*a–d*, *h*, *i*), (4.3*a–c*), (4.4*b–d*), with the above modifications. In addition, the local pressure expansion (4.5*a*) remains valid provided that in (4.6*a–c*) $\bar{M}_1, \bar{M}_2$ are replaced by $\bar{u}_1, \bar{u}_2$ respectively. Similarly, the local velocity expansions (4.7*a–c*) remain true provided that

$$G_{-1} = -\tilde{p}_1/\mathrm{i}\alpha\bar{u}_1, \quad H_{-1} = (f_{\bar{z}}\tilde{p}_1 - \tilde{p}_{0\bar{z}})/\mathrm{i}\alpha\bar{u}_1, \quad F_{-1} = -H_{-1\bar{z}}/\mathrm{i}\alpha \tag{C 2), (C 3), (C 4}$$

instead of (4.8*a–c*) in turn; also

$$G_0 = -\bar{u}_2 G_{-1}/\bar{u}_1 - 2\tilde{p}_2/\mathrm{i}\alpha\bar{u}_1, \tag{C 5}$$

$$H_0 = -\bar{u}_2 H_{-1}/\bar{u}_1 + (2f_{\bar{z}}\tilde{p}_2 - \tilde{p}_{1\bar{z}})/\mathrm{i}\alpha\bar{u}_1 \tag{C 6}$$

in this case.

Note added in proof. Professor S. N. Brown and Ms P. G. Brown have kindly pointed out that terms proportional to Y are missing in (B 17) in Appendix B, due to the double integration of (B 12). In consequence, $\mathscr{L}_1$ in (4.1) should be replaced by $Re^{-\frac{1}{12}}$

(with corresponding reductions in the wave amplitudes and vortex-flow variation for the critical layer in Appendix B), leaving the structure and equations of §4 intact except that (4.4*b*) should be replaced by

$$[\bar{w}_{\bar{y}}]_-^+ = \frac{2\pi(\frac{2}{3})^{\frac{2}{3}}\Gamma(\frac{1}{3})}{\Delta^5 a^{\frac{5}{3}}}\left\{\left(\frac{-7\Delta_{\bar{z}}}{2\Delta}-\frac{5a_{\bar{z}}}{3a}\right)|\tilde{p}_{\bar{z}}|^2+\partial_{\bar{z}}(|\tilde{p}_{\bar{z}}|^2)\right\}$$

($a \equiv \lambda\alpha\Delta^{-1}$), which imposes a jump condition on the vortex shear across the critical layer. The above jump applies for the incompressible regime, with a corresponding generalization to the compressible case. Also, relatively minor alterations follow in §5 and in (C 1) in Appendix C.

REFERENCES

Bassom, A. P. & Hall, P. 1990 *Stud. Appl. Maths* (in press).

Bennett, J. & Hall, P. 1987 *J. Fluid Mech.* **188**, 445.

Bennett, J., Hall, P. & Smith, F. T. 1991 *J. Fluid Mech.* **223**, 475.

Benney, D. & Chow, C. 1989 *Stud. Appl. Maths* **80**, 37.

Benney, D. & Lin, C. C. 1960 *Phys. Fluids* **3**, 657.

Blackaby, N. D. 1991 On viscous, inviscid and centrifugal instability mechanisms in compressible boundary layers, including non-linear vortex/wave interactions and the effects of large Mach number on transition. Ph.D. thesis, University of London.

Blennerhassett, P. J. & Smith, F. T. 1991 To be submitted for publication.

Bowles, R. I. 1989 Ph.D. Thesis, University of London.

Brown, S. N. & Smith, F. T. 1990 *J. Fluid Mech.* **219**, 499.

Bush, W. B. 1966 *J. Fluid Mech.* **25**, 51.

Cowley, S. J. & Hall, P. 1990 *J. Fluid Mech.* **214**, 17.

Craik, A. D. D. 1971 *J. Fluid Mech.* **50**, 393.

Davey, A. 1962 *J. Fluid Mech.* **14**, 336.

Duck, P. W. 1985 *J. Fluid Mech.* **160**, 465.

Fasel, H., Rist, U. & Konzelmann, U. 1987 *AIAA Paper* 87-1203.

Gajjar, J. S. B. 1989 Submitted for publication.

Gilbert, N. & Kleiser, L. 1986 In *Direct and Large Eddy Simulation of Turbulence* (ed. U. Schumann & R. Friedrich), pp. 1–18. Vieweg.

Gilbert, N. & Kleiser, L. 1988 In *Proc. Intl Seminar on Near-Wall Turbulence. Hemisphere.*

Hall, P. 1982 *J. Inst. Maths Applics.* **29**, 173–196.

Hall, P. 1983 *J. Fluid Mech.* **130**, 41–68.

Hall, P. 1988 *J. Fluid Mech.* **193**, 243.

Hall, P. & Lakin, W. D. 1988 *Proc. R. Soc. Lond.* A **415**, 421.

Hall, P. & Seddougui, S. 1989 *J. Fluid Mech.* **204**, 405.

Hall, P. & Smith, F. T. 1984 *Stud. Appl. Maths* **70**, 91.

Hall, P. & Smith, F. T. 1988 *Proc. R. Soc. Lond.* A **417**, 255.

Hall, P. & Smith, F. T. 1989 *Eur. J. Mech.* B **8**, 179.

Hall, P. & Smith, F. T. 1990 *Proc. ICASE Workshop on Instability and Transition*, Vol. II (ed. M. Y. Hussaini & R. G. Voigt), pp. 5–39. Springer.

Hama, F. R. & Nutant, J. 1963 In *Proc. Heat Transfer and Fluid Mech. Inst.* pp. 77–93. Stanford University Press.

Holden, M. S. 1985 *AIAA Paper* 85–0325.

Hoyle, J. M., Smith, F. T. & Walker, J. D. A. 1991 *Comput. Phys. Commun.* (in press).

Kachanov, Yu. S. & Levchenko, V. Yu 1984 *J. Fluid Mech.* **138**, 209.

Klebanoff, P. S., Tidstrom, K. D. & Sargent, L. M. 1962 *J. Fluid Mech.* **12**, 1.

KLEISER, L. & SCHUMANN, U. 1984 *Proc. ICASE Symp. on Spectral Methods* (ed. R. G. Voigt, D. Gottlieb, & M. Y. Hussaini), pp. 141–163. SIAM-CBMS.

LAURIEN, E. & KLEISER, L. 1989 *J. Fluid Mech.* **199**, 403.

LEE, R. S. & CHENG, H. K. 1969 *J. Fluid Mech.* **38**, 161–179.

MACK, L. M. 1975 *AIAA J.* **13**, 278–289.

MACK, L. M. 1984 *AGARD Rep.* 709.

MALIK, M. R. 1982 *NASA CR*-165925.

MALIK, M. R. 1987 *AIAA Paper* 87–1414.

MALKUS, W. 1956 *J. Fluid Mech.* **1**, 521.

NISHIOKA, M. & ASAI, M. 1984 In *Turbulence and Chaotic Phenomena in Fluids* (ed. T. Tatsumi), pp. 87–92. North-Holland.

NISHIOKA, M. & ASAI, M. 1985 *J. Fluid Mech.* **150**, 441.

NISHIOKA, M., ASAI, M. & IIDA, S. 1981 In *Transition and Turbulence* (ed. R. E. Meyer), pp. 113–126. Academic.

PERIDIER, V. J., SMITH, F. T. & WALKER, J. D. A. 1991*a* Vortex-induced boundary-layer separation. Part 1. The limit problem $Re \to \infty$. *J. Fluid Mech.* (in press).

PERIDIER, V. J., SMITH, F. T. & WALKER, J. D. A. 1991*b* Vortex-induced boundary-layer separation. Part 2. Unsteady interacting boundary-layer theory. *J. Fluid Mech.* (in press).

SEDDOUGUI, S., SMITH, F. T. & BOWLES, R. I. 1991 *Eur. J. Mech.* (in press).

SMITH, F. T. 1979*a* *Proc. R. Soc. Lond.* A **368**, 573.

SMITH, F. T. 1979*b* *Mathematika* **26**, 187.

SMITH, F. T. 1986 *J. Fluid Mech.* **169**, 353.

SMITH, F. T. 1988 *Mathematika* **35**, 256–273.

SMITH, F. T. 1989 *J. Fluid Mech.* **198**, 127.

SMITH, F. T. 1991 *Computers & Fluids* (to appear). (*Proc. R. T. Davis Memorial Symp., Cincinnati, 1987*).

SMITH, F. T. & BURGGRAF, O. R. 1985 *Proc. R. Soc. Lond.* A **399**, 25.

SMITH, F. T., DOORLY, D. J. & ROTHMAYER, A. P. 1990 *Proc. R. Soc. Lond.* A **428**, 255.

SMITH, F. T. & STEWART, P. A. 1987 *J. Fluid Mech.* **179**, 227.

SMITH, F. T. & WALTON, A. G. 1989 *Mathematika* **36**, Part 2, 262.

SPALART, P. R. & YANG, K. S. 1987 *J. Fluid Mech.* **178**, 345–365.

STEWARTSON, K. 1964 *The Theory of Laminar Boundary Layers in Compressible Fluids.* Oxford University Press.

STUART, J. T. 1960 *J. Fluid Mech.* **9**, 383.

THOMAS, A. S. W. 1987 In *Proc. 10th US Natl. Congress on Applied Maths*, pp. 436–444. ASME.

WALTON, A. G. 1991 Theory and computation of three-dimensional nonlinear effects in pipe flow transition. Ph.D. thesis, University of London.

WATSON, J. 1960 *J. Fluid Mech.* **9**, 371.

WILLIAMS, D. R. 1987 In *Stability of Time Dependent and Spatially Varying Flows* (ed. D. L. Dwoyer & M. Y. Hussaini), pp. 335–350. Springer.

WILLIAMS, D. R., FASEL, H. & HAMA, F. R. 1984 *J. Fluid Mech.* **149**, 179.

WRAY, A. A. & HUSSAINI, M. Y. 1984 *Proc. R. Soc. Lond.* A **392**, 393.

ZANG, T. A. & HUSSAINI, M. Y. 1986 *Appl. Math. Comput.* **19**, 359.

ZANG, T. A. & HUSSAINI, M. Y. 1987 In *Nonlinear Wave Interactions in Fluids* (ed. R. W. Miksad, T. R. Akylas, T. Herbert), pp. 131–145. ASME.

ZANG, T. A. & KRIST, S. E. 1989 *Theor. Comput. Fluid Dyn.* **1**, 41.